Table 1: Primer sequences

	forward primer	reverse primer
gSG 1F/R	atgcgaagagctgtgtcctg	tgccaccaaagaagaaagaa
gSG 2F/R	gcctccctcattccctctct	tcagagccagacagcaaagaa
gSG 3F/R	ggagaaatgcagaaaaggtggt	tgtgcacatgtatgcgcttt
gSG 4F/R	cagcacctattttgcaaattttataaatc	gcaccatgatgaagctggactc
gSG 5F/R	tagggttgacgtggcatgtg	tgtgtactccatggaatgttgtg
gSG 6F/R	gcctgctaatttgtaattgctttg	gcggaaagtcttgaaaataaagg
gSG 7F/R	ttttgtgcttcttttcctcatctc	cagtaggaggctgatctgtga
gSG 8F/R	ccttaactcttcgtctcccatctt	gcgtttacgtcccatccacgctgcc
gαDG 2F/R	tccaactcggggtagatgtttt	acttgaaaaggaaaagccacca
mSG 1F/7R	cattctgtctgtggtagagctcgg	gtttcagcatcaagcacaagcattcc
mSG 5F/8R	aaatggtagaagtccagaatcaaca	gcgtttacttcccatccacgctgc

527), H-E staining revealed marked replacement of muscle by adipose tissue along with increases in endomysial connective tissue. We also found a few muscle fibers that were remarkably different in size (data not shown). In spite of the clinical diagnosis of DMD, the immunostaining pattern for both dystrophin and merosin staining was completely normal. Unexpectedly, there was no staining for γ-sarcoglycan, while there was only a mild reduction for α-sarcoglycan and almost normal results for β- and δ-sarcoglycan (Figure 1). In order to confirm the γ-sarcoglycan deficiency, we looked for mutations in the SGCG gene. When PCR was used to amplify the eight exons that encompassed the regions of the SGCG gene, all regions other than exon 6 could be obtained. This suggests a homozygous deletion of exon 6 (Figure 2). To confirm this, we used RT-PCR to analyze the SGCG mRNA from the patient's muscle. Amplification of the fragment encompassing exons 5 to 8 resulted in a small-sized product. Subsequent sequencing of this product revealed a complete absence of the exon 6 sequence (data not shown). Therefore, we concluded that this patient had a homozygous deletion of exon 6 in the SGCG gene. In addition, both the patient's mother and father were found to carry this deletion in one allele (data not shown). Because the exon 6 deletion removes 73 bp (nt 506 - 578) from the mRNA, it was expected that a stop codon would appear in exon 7, thereby leading to γ-sarcoglycan deficiency. It became clear that this patient had LGMD2C rather than DMD.

In patient 2 (KUCG 280), H-E staining indicated excess variability of muscle fiber size, clusters of regenerating fibers, degenerating fibers, some acutely necrotic fibers, and scattered inflammatory cells. Immunohistochemistry revealed the absence of γ-sarcoglycan and a patchy reduction in α- and β-sarcoglycan. The staining patterns for dystrophin, δ-sarcoglycan, and merosin all appeared normal (Figure 1). Since the findings suggested γ-sarcoglycan deficiency, PCR amplification of the patient's genomic DNA was performed for all eight exons in the SGCG gene. Amplification of all fragments resulted in products that were of the expected size, and thus, subsequently could be used for direct sequencing. With the exception of exon 7, sequencing of the amplified products demonstrated a completely normal sequence. In exon 7, subcloning of an ambiguous sequence of the amplified product resulted in one clone with a completely normal sequence and a second clone that contained a novel single T nucleotide insertion between nt 602 and 603 within

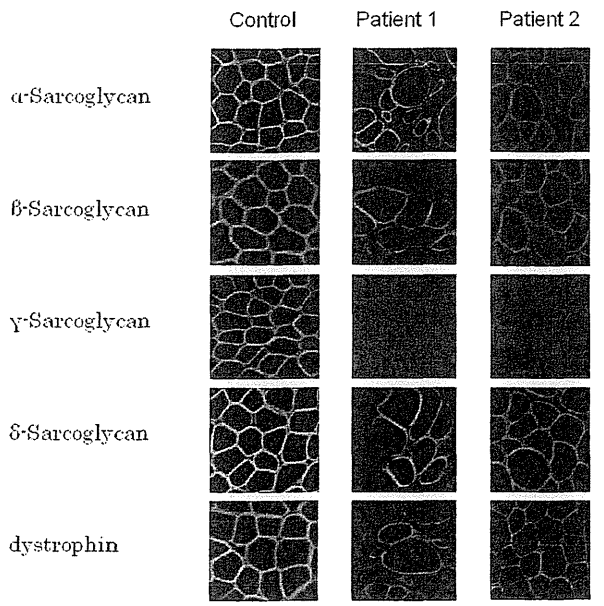

Figure 1 Immunostaining of skeletal muscle. Results of immunohistochemical examination using dystrophin, α-, β-, γ-, and δ-sarcoglycans and dystrophin antibodies are shown. There was clear staining of every protein along the plasma membrane in the control. In patient 1, γ-sarcoglycan was completely absent, and there was a mild reduction of α-sarcoglycan. Both β-sarcoglycan and δ-sarcoglycan were found to be almost entirely intact. There was clear staining of dystrophin in patient 1. In patient 2, γ-sarcoglycan was completely absent, and a patchy reduction in both α- and β-sarcoglycan was observed. Dystrophin, δ-sarcoglycan, and merosin staining patterns appeared normal.

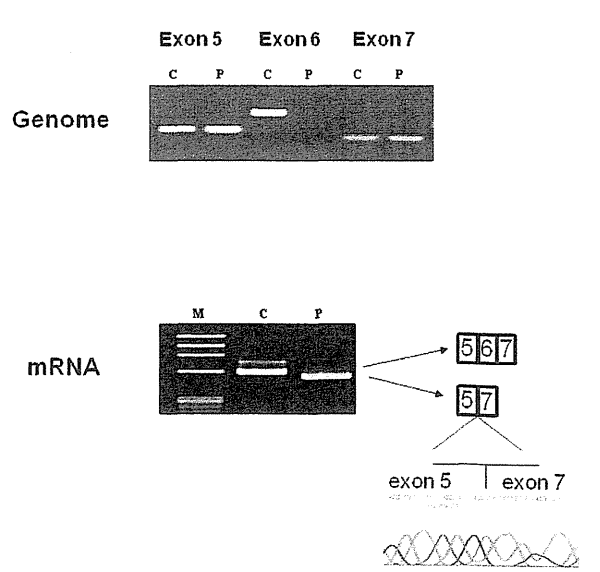

Figure 2 Mutation analysis of the SGCG gene in patient 1. Amplification products of exons 5, 6, and 7 are shown (c; control, p: patient) in the upper part of the figure. Although PCR amplification of eight exons of the SGCG gene was conducted, no products were obtained from the fragment encompassing exon 6 (Exon 6 p). For the other exons, the products of the SGCG gene met size expectations. Results of SGCG mRNA analysis are shown in the lower part of the figure. RT-PCR (c; control, p: patient) was used to analyze the muscle mRNA. The fragment encompassing exons 5 to 8 was amplified as a small-sized product in patient 1. Sequencing of the product showed a complete absence of exon 6. It was concluded that patient 1 had a homozygous deletion of exon 6 in the SGCG gene.

exon 7 (c.602_603insT). This mutation created a stop codon in exon 7. The patient's mother was heterozygous for this mutation, whereas the father had a normal exon 7 sequence (data not shown). Since patient 1 had a homologous deletion of exon 6 of the SGCG gene, we supposed that patient 2 carried this deletion in one allele. When semi-quantitative PCR amplification of exon 6 of the patient's SGCG gene was performed, the results showed nearly half the genomic dose for the exon 6 encompassing region, indicating a heterozygous deletion of exon 6 (Figure 3). Further analysis of the SGCG mRNA from the patient's muscle revealed two kinds of mRNA: one exhibited an exon 6 deletion and the other demonstrated the above-mentioned novel single nucleotide insertion within exon 7 (Figure 3). Therefore, the γ-sarcoglycan deficiency in this patient was caused by a hemizygous c.602-603insT in exon 7 along with the deletion of exon 6 on the other allele.

To date, our analysis of patients suspected to have DMD has revealed that two of the entire cohort examined can be regarded as having LGMD2C. Thus, the relative incidence of LGMD2C among Japanese patients suspected to have DMD can be calculated as 1 in 161 (2 of 324 patients = 0.6%). When the DMD incidence is taken into consideration for the overall population (1/3,500 males), the incidence of LGMD2C can be estimated as 1 per 560,000 or 1.8 per million.

Discussion

This is the first comprehensive study that has been able to definitively clarify the incidence of LGMD2C among patients suspected to have DMD. In our cohort of 324 Japanese children clinically diagnosed with DMD, two were diagnosed as having LGMD2C. The incidence of LGMD2C among this cohort was calculated as 1 in 161 (0.6%) and the incidence in the Japanese population was estimated at 1 per 0.56 million people. The relative proportions of all LGMDs, including LGMD2C, have been previously reported for various regions of the world [5,9]. However, these reports did not describe the relative prevalence of LGMD2C to DMD. The present study is the first to describe the incidence of LGMG2C in one race. The incidence of severe LGMDs was estimated to be 11.8% in a German study of patients with severe muscular dystrophy with early childhood onset [16] and about 8 to 12% in a Brazilian study of males with a clinical diagnosis of DMD [17]. In comparison, our results indicate a much

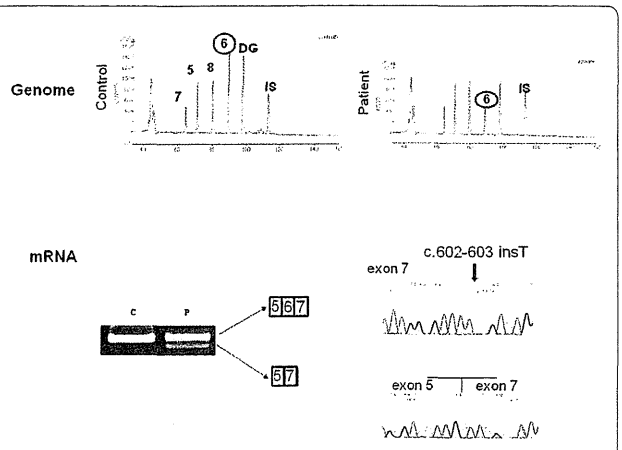

Figure 3 Mutation analysis of the SGCG gene in patient 2. Capillary electrophoretic patterns of the PCR products are shown in the upper portion of the figure. Five genomic regions were co-amplified in one PCR reaction, with the products separated using capillary electrophoresis. The position of each of the amplified products of exons 5, 6, 7, and 8 of the SGCG gene and exon 2 of the α-dystroglycan gene (DG) are marked. In patient 2, the peak area of exon 6 is nearly half that of the control, indicating a heterozygous deletion of exon 6. IS refers to a 1,500-bp marker. The amplified fragments that encompassed exons 5 to 8 of the SGCG mRNA are shown in the lower part of the figure (c; control, p; patient). Two different product sizes were obtained from the patient. Sequencing of the products disclosed that one exhibited a complete absence of exon 6, while the other included a nucleotide insertion in exon 7 (c.602_603insT). Thus, in this patient there was both a heterozygous nucleotide insertion in exon 7 and a heterozygous deletion of exon 6 of the SGCG gene.

lower incidence (0.6%) of LGMD2C among patients suspected to have DMD. However, the low prevalence of LGMD2C in Japanese is in accordance with the few reports that have examined LCMD2C patients from Japan [18,19]. Regardless of these differences, the potential presence of LGMD2C needs to be considered when making a differential diagnosis of DMD, even in Japan.

Although originally reported to be a severe autosomal recessive muscular dystrophy that resembles DMD, LGMD2C has since been reported to have a heterogenous clinical course, even with identical mutations [19]. Initially, both of our LGMD2C patients were tentatively diagnosed as having DMD, even though both patients showed only very mild muscle weakness during the original observation period. A clinical hallmark for differentiating DMD and LGMD2C involves the inheritance pattern. However, this is impossible to determine in sporadic cases in males. In the current cases, the failure to determine any dystrophin gene mutations that were responsible for DMD led to immunohistochemical examination of muscle tissue. Quite unexpectedly, we found normal staining for dystrophin in these patients (Figure 1). This finding proved to be the key for diagnosing the complete or near-complete absence of γ-sarcoglycan deficiency, which led to our using genetic analysis to definitively prove the γ-sarcoglycan deficiency.

It has been reported that residual sarcoglycan expression is highly variable, and that this makes it difficult to accurately predict the genotype [2,20]. In addition, both sarcoglycanopathy and DMD were reported to show weak staining of all types of sarcoglycan complexes [20]. On the other hand, patients with LGMD2C have been reported to show a significant reduction or a complete absence of γ-sarcoglycan staining in conjunction with reduced or only partially preserved staining of the other sarcoglycan proteins [2,5,9,21,22]. In the present two cases, we observed a marked reduction of γ-sarcoglycan, in addition to finding a reduction of staining intensity for other members of the sarcoglycan complex (Figure 1).

Since the maintenance of the carboxyl terminus of γ-sarcoglycan is important for both the processing and stability of the protein, mutations in the extracellular domain of γ-sarcoglycan can lead to an absence of protein expression [4]. While the most common cause of LGMD2C is thought to be a homozygous del521T in exon 6 of the SGCG gene, this mutation has not been reported in Japanese. However, in the current study we identified a novel c.602_603insT mutation. We identified a homozygous deletion of exon 6 of the SGCG gene in patient 1. We also identified the exon 6 deletion in three of four alleles in our two Japanese LGMD2C patients. This mutation has been previously reported to occur as a hemizygous condition in Japanese [19]. In Europe, this exon 6 deletion has been reported in both homozygous and hemizygous conditions [23]. Taken together, these previous findings suggest that exon 6 can be considered prone to deletions. Although our identification of the exon 6 deletion in one allele was initially difficult, we have now been able to successfully detect deletions in one allele by using semiquantitative PCR amplification (Figure 3). Therefore, use of this methodology may help to increase the mutation detection rate in patients suspected to have DMD, and in addition, help to correctly identify LGMD2C. Being able to successfully identify LGMD2C patients in the future will help to ensure correct DMD diagnosis and proper implementation of therapy in patients who do indeed have DMD.

Conclusion

This is the first comprehensive study to describe the prevalence of LGMD2C in one race from mutation study results on patients suspected to have DMD. The incidence of LGMD2C in the Japanese population was estimated to be 1 per 560,000.

Competing interests

The authors declare that they have no competing interests.

Authors' contributions

YO performed the molecular genetic studies, participated in the sequence alignment and drafted the manuscript. KI carried out the immunoassays. ZZ and HA participated in the sequence alignment. YT, MY, KM and TK participated in the design of the study. MM conceived of the study, and participated in its design and coordination and helped to draft the manuscript. All authors read and approved the final manuscript.

Acknowledgements

We would like to thank Ms. Kanako Yokoyama for her secretarial help. This work was supported by a Grant-in-Aid for Scientific Research (B) and Grant-in-Aid for Exploratory Research from the Japan Society for the Promotion of Science; a Health and Labour Sciences Research Grant for Research on Psychiatric and Neurological Diseases and Mental Health; and a research grant for Nervous and Mental disorders from the Ministry of Health, Labour, and Welfare.

Author Details

[1]Department of Pediatrics, Kobe University Graduate School of Medicine, Kobe 650-0017, Japan, [2]Department of Pathology and Applied Neurobiology, Graduate School of Medical Science, Kyoto Prefectural University of Medicine, Kyoto 602-8566, Japan and [3]Aichi Welfare Center for Persons with Developmental Disabilities, Aichi 480-0392, Japan

Received: 27 July 2009 Accepted: 30 March 2010
Published: 30 March 2010

References

1. Emery AEH: **Duchenne muscular dystrophy.** Oxford: Oxford University Press; 1993.
2. Bonnemann CG, Wong J, Jones KJ, Lidov HG, Feener CA, Shapiro F, Darras BT, Kunkel LM, North KN: **Primary gamma-sarcoglycanopathy (LGMD 2C): broadening of the mutational spectrum guided by the immunohistochemical profile.** *Neuromuscul Disord* 2002, **12**:273-280.
3. Ozawa E, Noguchi S, Mizuno Y, Hagiwara Y, Yoshida M: **From dystrophinopathy to sarcoglycanopathy: evolution of a concept of muscular dystrophy.** *Muscle & Nerve* 1998, **21**:421-438.
4. McNally EM, Duggan D, Gorospe JR, Bonnemann CG, Fanin M, Pegoraro E, Lidov HGW, Noguchi S, Ozawa E, Finkel RS, *et al.*: **Mutations that disrupt the carboxyl-terminus of g-sarcoglycan cause muscular dystrophy.** *Hum Mol Genet* 1996, **5**:1841-1847.
5. Guglieri M, Magri F, D'Angelo MG, Prelle A, Morandi L, Rodolico C, Cagliani R, Mora M, Fortunato F, Bordoni A, *et al.*: **Clinical, molecular, and protein correlations in a large sample of genetically diagnosed Italian limb girdle muscular dystrophy patients.** *Hum Mutat* 2008, **29**:258-266.
6. Kooi AJ van der, Barth PG, Busch HF, de Haan R, Ginjaar HB, van Essen AJ, van Hooff LJ, Howeler CJ, Jennekens FG, Jongen P, *et al.*: **The clinical spectrum of limb girdle muscular dystrophy. A survey in The Netherlands.** *Brain* 1996, **119**:1471-1480.
7. Emery AE: **Population frequencies of inherited neuromuscular diseases--a world survey.** *Neuromuscul Disord* 1991, **1**:19-29.
8. Georgieva B, Todorova A, Tournev I, Mitev V, Kremensky I: **C283Y gamma-sarcoglycan gene mutation in the Bulgarian Roma (Gypsy) population: prevalence study and carrier screening in a high-risk community.** *Clin Genet* 2004, **66**:467-472.
9. Moore SA, Shilling CJ, Westra S, Wall C, Wicklund MP, Stolle C, Brown CA, Michele DE, Piccolo F, Winder TL, *et al.*: **Limb-girdle muscular dystrophy in the United States.** *J Neuropathol Exp Neurol* 2006, **65**:995-1003.
10. Matsuo M: **Duchenne/Becker muscular dystrophy: from molecular diagnosis to gene therapy.** *Brain Dev* 1996, **18**:167-172.
11. Takeshima Y, Yagi M, Wada H, Ishibashi K, Nishiyama A, Kakumoto M, Sakaeda T, Saura R, Okumura K, Matsuo M: **Intravenous infusion of an antisense oligonucleotide results in exon skipping in muscle dystrophin mRNA of Duchenne muscular dystrophy.** *Pediatr Res* 2006, **59**:690-694.
12. Welch EM, Barton ER, Zhuo J, Tomizawa Y, Friesen WJ, Trifills P, Paushkin S, Patel M, Trotta CR, Hwang S, *et al.*: **PTC124 targets genetic disorders caused by nonsense mutations.** *Nature* 2007, **447**(7140):87-91.
13. Matsuo M, Masumura T, Nishio H, Nakajima T, Kitoh Y, Takumi T, Koga J, Nakamura H: **Exon skipping during splicing of dystrophin mRNA precursor due to an intraexon deletion in the dystrophin gene of Duchenne muscular dystrophy Kobe.** *J Clin Invest* 1991, **87**:2127-2131.
14. Tran VK, Zhang Z, Yagi M, Nishiyama A, Habara Y, Takeshima Y, Matsuo M: **A novel cryptic exon identified in the 3' region of intron 2 of the human dystrophin gene.** *J Hum Genet* 2005, **50**:425-433.
15. Yagi M, Takeshima Y, Wada H, Nakamura H, Matsuo M: **Two alternative exons can result from activation of the cryptic splice acceptor site deep within intron 2 of the dystrophin gene in a patient with as yet asymptomatic dystrophinopathy.** *Hum Genet* 2003, **112**:164-170.
16. Stec I, Kress W, Meng G, Muller B, Muller CR, Grimm T: **Estimate of severe autosomal recessive limb-girdle muscular dystrophy (LGMD2C, LGMD2D) among sporadic muscular dystrophy males: a study of 415 familes.** *J Med Genet* 1995, **32**:930-933.
17. Vainzof M, Pavanerllo R, Pavanello-Filho I, Rapaport D, Passo-Bueno M, Zubrzycka GEE, Bulman D, Zatz M: **Screening of male patients with autosomal recessive Duchenne dystrophy through dystrophin and DNA studies.** *Am J Med Gent* 1991, **39**:38-41.
18. Hayashi YK, Mizuno Y, Yoshida M, Nonaka I, Ozawa E, Arahata K: **The frequency of patients with 50-kd dystrophin-associated glycoprotein (50DAG or adhalin) deficiency in a muscular dystrophy patient population in Japan: immunocytochemical analysis of 50DAG, 43DAG, dystrophin, and utrophin.** *Neurology* 1995, **45(3 Pt 1)**:551-554.
19. Takano A, Bonnemann CG, Honda H, Sakai M, Feener CA, Kunkel LM, Sobue G: **Intrafamilial phenotypic variation in limb-girdle muscular dystrophy type 2C with compound heterozygous mutations.** *Muscle Nerve* 2000, **23**:807-810.
20. Klinge L, Dekomien G, Aboumousa A, Charlton R, Epplen JT, Barresi R, Bushby K, Straub V: **Sarcoglycanopathies: Can muscle immunoanalysis predict the genotype?** *Neuromuscul Disord* 2008, **18**:934-941.
21. Hack AA, Lam MY, Cordier L, Shoturma DI, Ly CT, Hadhazy MA, Hadhazy MR, Sweeney HL, McNally EM: **Differential requirement for individual sarcoglycans and dystrophin in the assembly and function of the dystrophin-glycoprotein complex.** *J Cell Sci* 2000, **113(Pt 14)**:2535-2544.
22. Vainzof M, Passos-Bueno MR, Canovas M, Moreira ES, Pavanello RCM, Marie SK, Anderson LVB, Bonnemann CG, McNally EM, Nigro V, *et al.*: **The sarcoglycan complex in the six autosomal recessive limb-girdle muscular dystrophies.** *Hum Mol Genet* 1996, **5**:1963-1969.
23. Duncan DR, Kang PB, Rabbat JC, Briggs CE, Lidov HG, Darras BT, Kunkel LM: **A novel mutation in two families with limb-girdle muscular dystrophy type 2C.** *Neurology* 2006, **67**:167-169.

Pre-publication history

The pre-publication history for this paper can be accessed here:
http://www.biomedcentral.com/1471-2350/11/49/prepub

doi: 10.1186/1471-2350-11-49
Cite this article as: Okizuka *et al.*, Low incidence of limb-girdle muscular dystrophy type 2C revealed by a mutation study in Japanese patients clinically diagnosed with DMD *BMC Medical Genetics* 2010, **11**:49

Molecular Vision 2010; 16:2590-2597 <http://www.molvis.org/molvis/v16/a277>
Received 28 July 2010 | Accepted 2 December 2010 | Published 7 December 2010

Molecular characterization of the 5′-UTR of retinal dystrophin reveals a cryptic intron that regulates translational activity

Ikuko Kubokawa, Yasuhiro Takeshima, Mitsunori Ota, Masahiro Enomoto, Yo Okizuka, Takeshi Mori, Noriyuki Nishimura, Hiroyuki Awano, Mariko Yagi, Masafumi Matsuo

Department of Pediatrics, Graduate School of Medicine, Kobe University, Kobe, Japan

Purpose: Mutations in the dystrophin (*DMD*) gene cause Duchenne or Becker muscular dystrophy (DMD/BMD). *DMD* contains a retina-specific promoter in intron 29. The short R-dystrophin transcript from this promoter has a retina-specific exon 1 (R1) joined to exon 30 of the *DMD* gene. It has been claimed that this is responsible for the ophthalmological problems observed in DMD/BMD. This research characterizes the structure of the 5′-untranslated region (5′-UTR) of human R-dystrophin.

Methods: The 5′-UTR of the human R-dystrophin transcript was amplified from human retina and 20 other human tissue RNAs by reverse transcription polymerase chain reaction (RT–PCR). Amplified products were identified by sequencing. The translational activities of transcripts bearing differing 5′-UTRs were measured using a dual luciferase assay system.

Results: RT–PCR amplification of the R-dystrophin transcript from the retina using a conventional primer set revealed one product comprising exon R1 and exons 30 to 32 (R-dys α). In contrast, three amplified products were obtained when a forward primer at the far 5′-end of exon R1 was employed for RT–PCR. R-dys α, and a shorter form in which 98 bp was deleted from exon R1 (R-dys β), were the two major products. A minor, short form was also identified, in which 143 bp was deleted from exon R1 (R-dys γ). The two primary retinal products (R-dys α and β) encoded an identical open reading frame. The 98 bp deleted in R-dys β was identified as a cryptic intron that was evolutionarily acquired in higher mammals. The shorter R-dys β was expressed in several tissues with a wide range in expression level, while R-dys α was retina specific. The 5′-UTRs of R-dys α and β were examined for translational activity using a dual luciferase assay system. Unexpectedly, the 5′-UTR of R-dys β showed lower translational activity than that of R-dys α. This lower activity was presumed to be due to the removal of internal ribosome entry sites by activation of cryptic intron splicing.

Conclusions: An evolutionarily-acquired cryptic intron was identified in the 5′-UTR of the human R-dystrophin transcript. The two abundant R-dystrophin transcripts in the retina showed different translational activities in vitro owing to their differential splicing of the cryptic intron. This evolutionarily-acquired alternative splicing may act as a molecular switch that regulates translation of the R-dystrophin transcript.

The dystrophin (*DMD*) gene is responsible for the most common inherited muscle diseases, Duchenne and Becker muscular dystrophies (DMD/BMD). *DMD* is the largest known human gene, spanning more than 2.5 Mb on chromosome Xp21.2, and comprises 79 exons and large introns. At least eight alternative promoters/first exons are scattered among the introns. Four tissue-specific promoters at the 5′-end of the gene express full-length dystrophin, while four internal promoters express smaller isoforms containing unique first exons that are activated in a tissue-specific manner [1–3].

An alternative promoter/first exon located within intron 29 is strongly expressed in the retina. The first exon (R1) splices to exon 30 of the *DMD* gene to encode R-dystrophin [3,4]. Exon R1 is 236 bp long and encodes 13 retina-specific amino acids, leaving 197 bp as the 5′-untranslated region (5′-UTR) [4]. This protein has been identified as human R-dystrophin by western blotting of retinal dystrophin proteins (Dp260) [5]. In addition, a single sequence with a 143-bp deletion in exon R1 has been deposited in GenBank (NM_004011.3). This variant contains a 95 bp exon R1 encoding a unique 16 amino acids of N-terminal end. R-dystrophin has been shown to be involved in the commitment of synaptic maturation and attachment of the retina to the vitreous [6–8]. Furthermore, R-dystrophin has been categorized as a cytolinker in skeletal muscle because it organizes costameric microtubules in the skeletal muscle of transgenic mdx mice expressing R-dystrophin [9].

DMD and BMD have been described to have ophthalmological complications [8,10,11]. A reduced electroretinogram (ERG) b-wave was identified in DMD and considered a direct consequence of dystrophin deficiency [4, 5,8,10]. A subset of DMD patients with deletions downstream of exon 30, affecting the splicing and transcription of R-dystrophin, exhibit a red-green color vision defect, while DMD patients who have dystrophin mutations upstream of exon 30 have seemingly normal color vision [11]. This color

Correspondence to: Masafumi Matsuo, Department of Pediatrics, Graduate School of Medicine, Kobe University, 7-5-1 Kusunokicho, Chuo-ku, Kobe 650-0017, Japan; Phone: +81-78-382-6080; FAX: +81-78-382-6098; email: matsuo@kobe-u.ac.jp

vision defect is likely caused by a loss of R-dystrophin. Thus, both molecular and clinical findings suggest an important role for R-dystrophin.

Alternative splicing is a source of genetic variation, and more than 95% of genes have at least one alternative splicing site [12]. Alternative splicing within the protein-coding region attracts much attention, because it is likely to directly impact protein function. In contrast, alternative splicing in 5′-UTRs has not been characterized as well. It is known that the 5′-UTR is a major site of translational regulation through internal ribosome entry sites (IRES) [13–15] or upstream AUG (uAUG) motifs [16]. Abnormalities in the 5′-UTR can be pathogenic [13,17]. Alternative splicing in the 5′-UTR has been shown to play a significant role in gene function [18]. However, the 5′-UTR of the human R-dystrophin transcript has not been well characterized.

Here, we identified an evolutionarily-acquired alternative splicing pathway in the 5′-UTR of the R-dystrophin transcript. We showed that transcripts with an alternatively-spliced 5′-UTR have a lower translational activity than those with a non-spliced 5′-UTR.

METHODS

Transcript analysis: RT–PCR amplification was conducted to examine the R-dystrophin transcript. Human total RNAs from retina and 20 other tissues (adrenal gland, colon, cerebellum, whole brain, fetal brain, fetal liver, heart, kidney, liver, lung, placenta, prostate, salivary gland, skeletal muscle, spleen, testis, thymus, thyroid gland, trachea, and uterus) were obtained from a human total RNA Master Panel II (Clontech Laboratories, Inc., Mountain View, CA). cDNA was synthesized as described previously [19] from 2.5 μg of each total RNA. A retinal promoter-derived transcript spanning exon R1 to exon 32 was PCR amplified using the following primers: forward primer, RdysF-N119: 5′-ATG CAG AGA TCC CTG ATC CTA TAG-3′ [4] and reverse primer on exon 32, 2F: 5′-TTC CAC ACT CTT TGT TTC CAA TG-3′. To extend the amplified region, another forward primer was used at the 5′-end of exon R1 (Rdys-F: 5′-GGA GGA ACA TTC GAC CTG AG-3′). PCR amplification was performed in a total volume of 20 μl, containing 2 μl of cDNA, 2 μl of 10× ExTaq buffer (Takara Bio, Inc., Shiga, Japan), 0.5 U of ExTaq polymerase (Takara Bio, Inc.), 500 nM of each primer and 250 μM dNTPs (Takara Bio, Inc.). Twenty-eight cycles of amplification were performed on a Mastercycler Gradient PCR machine (Eppendorf, Hamburg, Germany) using the following conditions: initial denaturation at 94 °C for 5 min, subsequent denaturation at 94 °C for 0.5 min, annealing at 59 °C for 0.5 min and extension at 72 °C for 1 min. Amplified PCR products were electrophoresed on a 2% agarose gel with a low molecular weight DNA standard (ϕX174-HaeIII digest; Takara Bio, Inc.), and stained with ethidium bromide.

PCR-amplified bands were excised from the gel with a sharp razor, pooled and purified using a QIAGEN gel extraction kit (QIAGEN, Inc., Hilden, Germany), according to the manufacturer's instructions. Purified products were subcloned into the pT7 blue T vector (Novagen, Inc., San Diego, CA), and sequenced using a Taq dye terminator cycle sequence kit (Life Technologies Corp., Carlsbad, CA) with an automatic DNA sequencer (3130 Genetic Analyzer; Life Technologies Corp.), as described previously [20]. RT–PCR products were semi-quantified using a DNA 1000 LabChip kit on an Agilent 2100 Bioanalyzer (Agilent Technologies, Santa Clara, CA).

To check the integrity and concentration of the cDNA, the glyceraldehyde 3-phosphate dehydrogenase (*GAPDH*) gene was also RT–PCR amplified, as described previously [21].

Translational activity assay:

Construction of plasmids—To measure the translational activity of the 5′-UTR of dystrophin transcripts, dual-luciferase reporter assays using the psiCHECK-2 vector (Promega Corp., Madison, WI), which allows simultaneous expression of *Renilla* and firefly luciferase from a single plasmid, were conducted in HEK293 cells. The 5′-UTR sequences of R-dys α (α5′-UTR) and β (β5′-UTR) were inserted into the *Renilla* luciferase gene. Before inserting the 5′-UTR sequences into the psiCHECK-2 vector, the ATG of the *Renilla* luciferase was mutated to TTG, named psiCHECK-2-TTG, so that the *Renilla* luciferase expression would be driven by the primary ATG initiation codon of the gene under investigation. The 5′-UTR sequences, up to and including the primary ATG initiation codon, were PCR amplified. The amplified products were cloned and ligated into the NheI site directly preceding the *Renilla* luciferase gene in the plasmid psiCHECK-2-TTG.

The α5′-UTR was PCR amplified using the primers H-Dp260Ex1-F: 5′-cgc *gct agc* TAA TGA GAT CAG GAG GAA CA-3′ and H-Dp260Ex1-α: 5′-cgc *gct agc* CTC ATT CAG CTC TGT TGA TA-3′; the β5′-UTR was amplified using H-Dp260Ex1-F and H-Dp260Ex1-β: 5′-cgc *gct agc* CTC ATT CAG CTA TTA AGG AA-3′. Upper case letters corresponded to sequences of the 5′-UTR. Lower case letters were sequences attached to create an NheI cut site (*gct agc*).

Luciferase activity assay—HEK293 cells were grown at 37 °C in a humidified atmosphere containing 5% CO_2 in Dulbecco's modified Eagle's medium (Sigma-Aldrich Corp., St Louis, MO) supplemented with 10% fetal bovine serum (Life Technologies Corp.) and 1% PSN antibiotic mixture (Life Technologies Corp.). HEK293 cells were seeded at 4×10^5 cells per well in 12-well dishes. After overnight incubation, the cells grew to approximately 80% confluency and 800 ng of each of the three vector constructs (the unmodified plasmid psiCHECK-2-TTG and the plasmids psiCHECK-2-α and -β) were transfected into the cells using Lipofectamine™ 2000 (Life Technologies Corp.). Twenty-four h after transfection, cells were washed with phosphate-buffered saline and resuspended in Passive Lysis Buffer

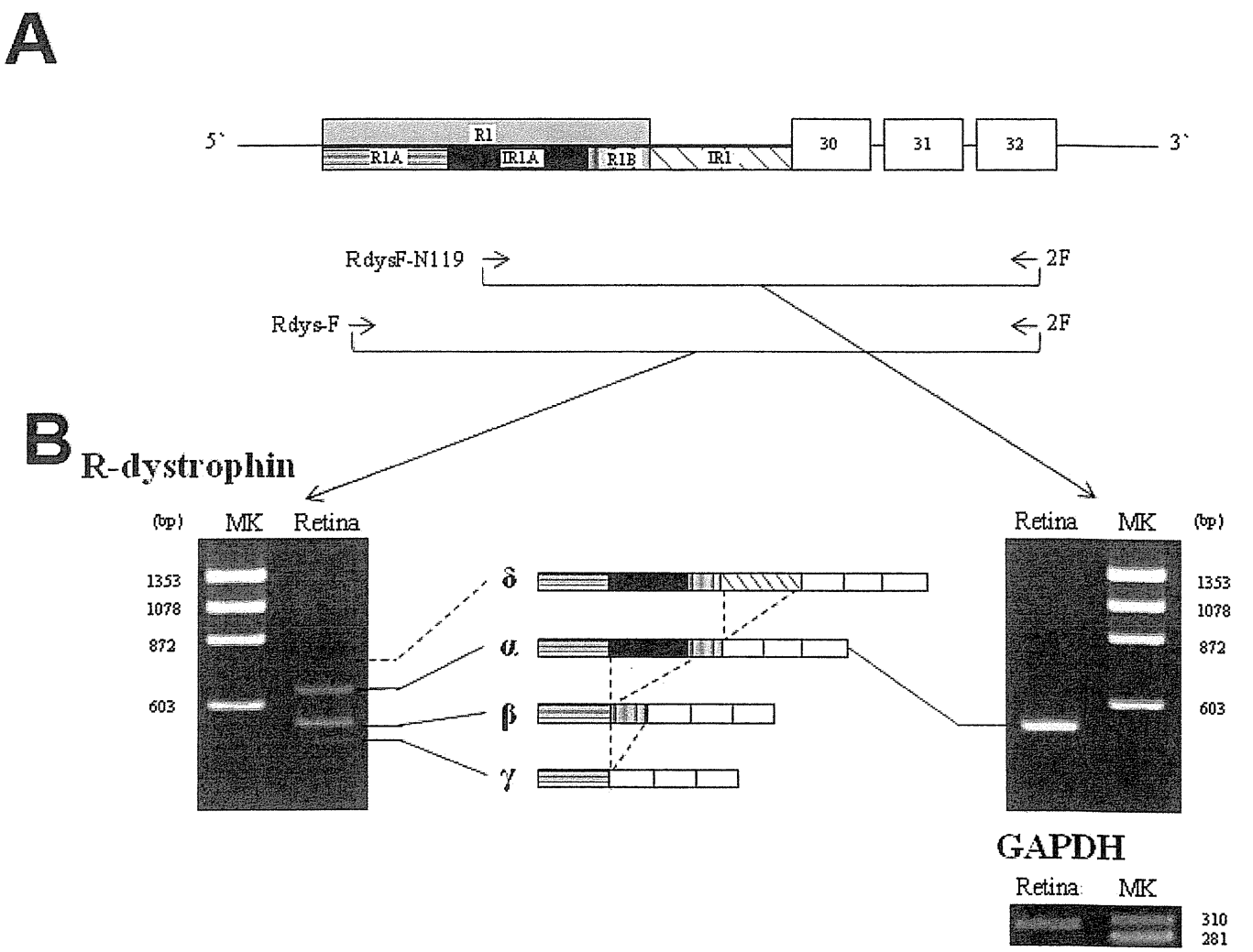

Figure 1. Reverse transcription polymerase chain reaction (RT–PCR) amplification of the R-dystrophin transcript. **A**: Schematic description of the region encompassing exons R1 to 32 of the dystrophin (*DMD*) gene. RT–PCR primers (RdysF-N119, Rdys-F and 2F) are shown as horizontal arrows. Boxes and bars indicate exons and introns, respectively. Exon/intron structures are described according to previous studies and the present study above and below the line, respectively. In this study, exon R1 is divided into three segments: the boxes labeled R1A (horizontal-lined), IR1A (black) and R1B (vertical bold-lined) represent exon R1A (93 bp), intron R1A (98 bp) and exon R1B (45 bp), respectively. Intron R1 was also incorporated into the mRNA (oblique-lined box). Numbers within the boxes indicate the exon number. The actual lengths of exon R1 and intron R1 are 236 bp and 105 bp, respectively. **B**: RT–PCR-amplified products of the fragment encompassing exons R1 to 32. Amplification from the retina using the conventional primer RdysF-N119 revealed one clear band of 529 bp (R-dys α; right). In contrast, RT–PCR amplification using the outer forward primer Rdys-F revealed three bands: two major products of 636 bp and 538 bp (R-dys α and β, respectively) and one weak product of 493 bp (R-dys γ; left). In addition, sequencing of subclones revealed an additional, larger product (R-dys δ). The exon structure of each product is described in the middle of each panel. The four R-dystrophin transcripts are shown by four bars. A fragment of *GAPDH* (302 bp) was amplified as a control (bottom). MK refers to the size marker (φX174 HaeIII digest).

(Promega Corp.). The firefly and *Renilla* luciferase activities were measured using a dual-luciferase reporter assay kit (Promega Corp.) with a plate reader (Fluoroskan Ascent FL; Thermo Fisher Scientific., Waltham, MA), according to the manufacturer's instructions. All experiments were performed in triplicate. To account for nonspecific effects on reporter plasmids, experimental results were expressed as a normalized ratio. The ratio of *Renilla* and firefly luciferase activity was normalized against the unmodified plasmid psiCHECK-2-TTG. The relative ratio of *Renilla*/firefly luciferase activity determined from cells transfected with the plasmid psiCHECK-2-α was set at 1 and was compared with that determined from the plasmid psiCHECK-2-β.

Analysis: The probability scores for the splice acceptor and donor sites were calculated as described previously [22]. Statistical significance was examined using Student's *t* test using GraphPad Prism software, version 5.02 (GraphPad Software Inc., San Diego, CA). A significant difference was

Figure 2. Genomic sequence of exon R1. **A**: Features of exon R1 (236 bp; GenBank NW_001842360.1). The 98-bp sequence, deleted in some transcripts and presumed to be a cryptic intron, is marked by a box. This sequence starts with GT and ends with AG (shaded). Bars below the sequence indicate internal ribosome entry sites. Dots over the ATG codons indicate a translation start site. **B**: Consensus dinucleotide sequences for the cryptic intron. The AG and GT splice consensus dinucleotides are present in humans and other mammals, including chimpanzee, orangutan and rhesus macaque. The mouse and rat genomic sequences contain GT/AA and AT/AA, respectively.

described, if the p value was less than 0.05. The secondary structure of the 5′-UTR was analyzed using Mfold, version 3.2. Internal ribosome entry sites (IRESs) were analyzed using IRESite.

RESULTS

Retinal dystrophin transcript: To characterize the 5′-UTR of the R-dystrophin transcript, a region from exon R1 to exon 32 was RT–PCR amplified from human retina RNA using a conventional forward primer on exon R1 (RdysF-N119) and a reverse primer on exon 32 (2F). One clear PCR-amplified product was obtained that comprised exons R1, 30, 31, and 32 (R-dys α) (Figure 1), as described previously [4]. This agreed with the current understanding of retinal dystrophin [11].

To examine the full length of exon R1, the same region was amplified using an outer forward primer (Rdys-F), 107 bp upstream of RdysF-N119 and located at the far 5′-end of exon R1. Three amplified products were visualized on agarose gels, with two major products and one minor product (Figure 1). Among the two major products, the longer product was identical to R-dys α. The shorter major product had the same exon content as R-dys α but had a 98-bp deletion within exon R1 located 45 bp upstream of the 3′-end of exon R1 (R-dys β; Figure 1). R-dys β was a novel variant of the R-dystrophin transcript. Because the ATG start codon is present within the common 45-bp region, the translational reading frame of both R-dys α and β was identical. R-dys β was expressed at a similar level to R-dys α in the retina, and it was speculated that the R-dys β may be physiologically important. The minor PCR band was identified to have a 143-bp deletion in exon R1 that shortened it to 93 bp (R-dys γ; GenBank NM_004011.3). In addition to the three visible products, a clone of 741 bp was identified by sequencing of subclones. This clone retained a 105-bp intron R1 between exons R1 and 30 (R-dys δ; Figure 1). This is suggested to be an immature mRNA transcribed from the R-dystrophin promoter.

Alternative splicing of the 5′-UTR of R-dystrophin: The difference between the two major retinal transcripts (R-dys α and β) was the absence or presence of the 98-bp sequence from their 5′-UTRs. Examination of this sequence revealed GT and AG dinucleotides at its 5′- and 3′-end, respectively (Figure 2). The probability scores for these dinucleotides to act as splice donor (GT) or acceptor (AG) sites were calculated as 0.76 and 0.93, respectively. These values were within the ranges of scores for the rest of *DMD* [23]. It was concluded that the 98-bp region is a novel cryptic intron embedded within exon R1. As a result, the 236-bp exon R1 can be divided into three segments: the 93-bp exon R1A, the 98-bp intron R1A and the 45-bp exon R1B (Figure 1 and Figure 2). The difference between R-dys α and β was thus caused by alternative splicing of intron R1A.

Alternative splicing of intron R1A has not been described in previous reports [4,24]. It was found that the cryptic intron R1A was evolutionarily acquired in humans but is not present in rodents, in which intensive studies on R-dystrophin have been conducted [25]. The mouse and rat genomic sequences corresponding to the human donor and acceptor sites of intron R1A have GT/AA and AT/AA, respectively, compared with GT/AG in humans (underlining indicates a mismatched nucleotide; Figure 2). Evolutionarily higher animals,

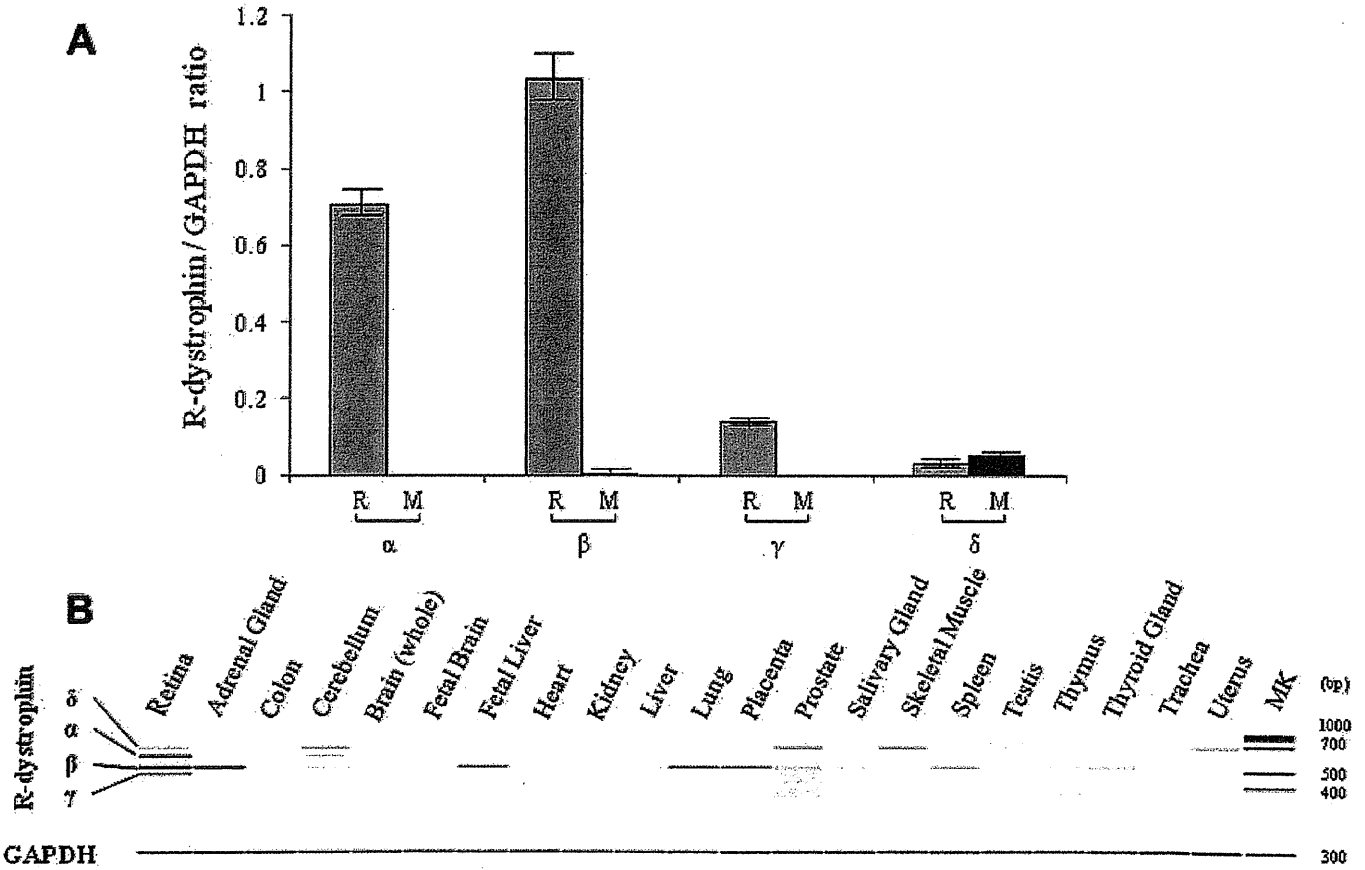

Figure 3. R-dystrophin variants in human tissues. **A**: Semi-quantitative analysis of R-dystrophin variants in the retina and the skeletal muscle. The ratio of each variant/GAPDH in the retina (R) and the skeletal muscle (M) are shown. A fragment comprising exons R1 to 32 was RT–PCR amplified from the retina and the skeletal muscle and semi-quantitated. The value was obtained by three quantifications and shown as mean±SD. In the retina (R), strong expression of R-dys α (α) and β (β) was observed. However, no significant difference between R-dys α and β was observed (0.70±0.05 and 1.03±0.16, respectively). In the skeletal muscle (M), R-dys α, β and γ (γ) were not detected but R-dys δ (δ) was observed at the quite low level. **B**: RT–PCR amplified products are shown. A fragment comprising exons R1 to 32 was RT–PCR amplified from 21 human tissues. Four products were obtained from the retina (R-dys α, β, γ, and δ) but R-dys α and β were the main products. R-dys α was also identified weakly in the cerebellum. R-dys β was present in several tissues including the adrenal gland. MK refers to the size marker (DNA 1000 Markers).

including the chimpanzee, orangutan and rhesus macaque, have the same sequence as humans in this region (Figure 2).

Tissue distribution of R-dystrophin variants: To examine the tissue expression patterns of the four variants of the R-dystrophin transcript, RT–PCR amplification using an outer forward primer was conducted in 21 human tissue RNAs. Semi-quantitative analysis was conducted in the retina and the skeletal muscle where retina- and muscle-specific promoters were active, respectively (Figure 3). In the retina, four variants could be detected, but R-dys α and β were the two main products. Expression levels of R-dys α and β were not significantly different. In the skeletal muscle, R-dys α, β, and γ were not detected but R-dys δ was marginally amplified. Unexpectedly, R-dys β, the shorter retinal product, was clearly amplified not only in the retina but also in the adrenal gland (Figure 3). Furthermore, R-dys β was detected weakly in the fetal liver, the lung, the placenta and the spleen. Expression of R-dys α was observed strongly in the retina and weakly in the cerebellum but not in any other tissues. It is interesting that R-dys α was detected weakly in the cerebellum (Figure 3) because R-dys α has been proposed to have a neuron-specific function [6–8].

Translational differences mediated by the 5′-UTRs of R-dys α and β: Although R-dys α and R-dys β encode an identical protein, they may be differentially translated in human tissues, because of their differing 5′-UTRs (α5′-UTR and β5′-UTR, respectively). Using a dual luciferase assay system, the translational activity of the β5′-UTR was significantly lower than that of the α5′-UTR (0.71±0.01 versus 1.00±0.01) (Figure 4). It was concluded that R-dys β is translated at a lower level than R-dys α, even though it is more widely expressed. Thus, R-dys α was considered more important in regards to protein production.

To investigate the mechanism providing the translational difference between R-dys α and β, their 5′-UTRs were examined for upstream open reading frames (uORFs) [26, 27] or secondary structure [28], but no clear explanation was obtained. When IRESs, which are considered to regulate translation [29,30], were analyzed, four IRES motifs were identified within the 98-bp intron R1A, and four were identified within the 93-bp exon R1A (Figure 2). Because intron R1A was rich in IRES motifs, R-dys β, which lacks intron R1A, was considered weak for translational activity.

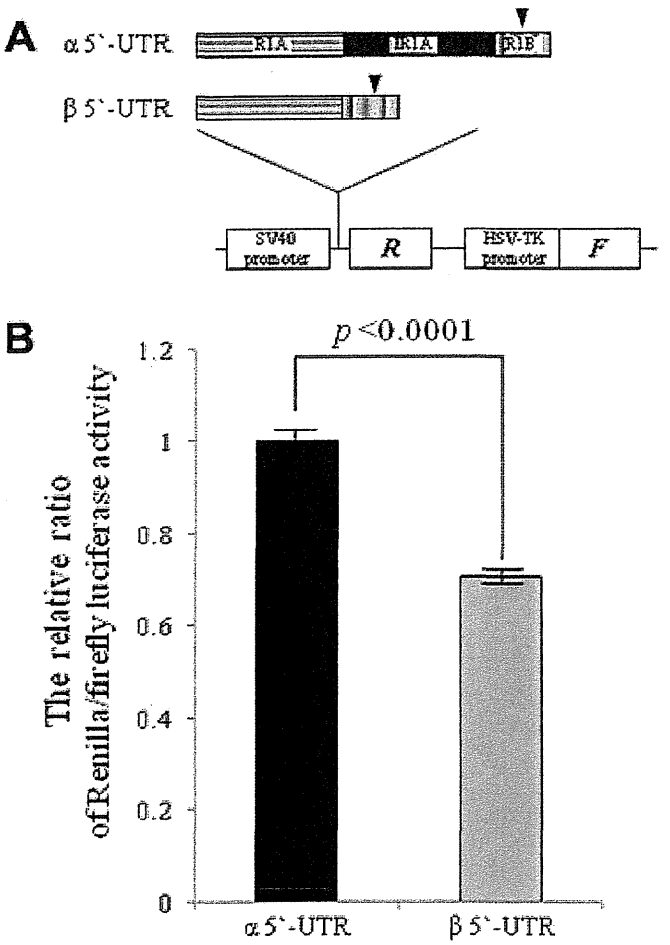

Figure 4. Translational activity of the 5′-UTR. **A**: Structure of the expression vector and inserted sequence. The psiCHECK-2 PCR vector is described (bottom). This vector contains the *Renilla* (*R*) and firefly (*F*) luciferases as the upstream and downstream cistrons, respectively. Both the α5′-UTR and the β5′-UTR were amplified (upper and middle, respectively) and inserted into the cloning site. Before inserting the 5′-UTR sequences into the psiCHECK-2 vector, the ATG of the *Renilla* luciferase was mutated to TTG, so that the *Renilla* luciferase expression would be driven by the primary ATG initiation codon (reverse triangle) of the gene under investigation. **B**: Luciferase activity. Three vector constructs (the unmodified plasmid psiCHECK-2-TTG and plasmids psiCHECK-2-α and -β) were transfected into HEK293 cells, and the firefly and *Renilla* luciferase activities were measured 24 h after transfection. All experiments were performed in triplicate. The ratio of *Renilla* and firefly luciferase activity was normalized against the unmodified plasmid psiCHECK-2-TTG. The relative ratio of *Renilla*/firefly luciferase activity determined from cells transfected with the plasmid psiCHECK-2-α was set at 1. The relative ratio of *Renilla*/firefly luciferase activity was significantly lower for the β5′-UTR than for the α5′-UTR (0.71±0.01 and 1.00±0.01, respectively).

DISCUSSION

In this study of the 5′-UTR of the R-dystrophin transcript, four different transcripts were identified in human retina (Figure 1). Two (R-dys α and γ) were previously known (GenBank, NM_004012.3 and NM_004011.3, respectively), and two new transcripts (R-dys β and δ) were cloned. Alternative splicing was shown to provide diversity in the transcripts produced from the retinal promoter, and a new, evolutionarily-acquired intron was identified within exon R1 (Figure 2). Among the four transcripts, two (R-dys α and β) were the primary products in the retina (Figure 1); these encode an identical open reading frame but have different 5′-UTRs, depending on the pattern of intron R1A splicing. It is proposed that splicing of the cryptic intron R1A in the 5′-UTR is a key regulator of the physiologic roles of these variants.

Considering that R-dys β was expressed in several human tissues (Figure 3), the production of R-dys β was considered the default pathway for the R-dystrophin transcript. It is supposed that an unidentified retina-specific factor shifts this default pathway to include the cryptic intron R1A in the retina, thereby producing R-dys α. R-dys α has a higher translational activity than R-dys β, at least in vitro (Figure 4), which produces R-dystrophin in the retina.

Intron R1A was found to have been acquired during evolution between rodents and primates (Figure 2), suggesting a higher physiologic role for the alternative splicing of cryptic intron R1A. Important roles for alternative splicing in the 5′-UTR have been demonstrated in the regulation of translation in certain human genes [12,13,18,27]. The β5′-UTR, without intron R1A, showed lower translational activity than the α5′-UTR in a dual luciferase assay (Figure 4). This result is contrary to the understanding that a long 5′-UTR suppresses translation by increasing the energy that a navigating ribosome needs to reach the AUG through a highly structured 5′-UTR, stable secondary structures or multiple uORFs [17]. Intron R1A retained in the α5′-UTR seemed to increase translation of R-dys α by virtue of multiple IRESs (Figure 4). It is known that mRNAs encoding proteins involved in cell growth, proliferation and apoptosis have structured 5′-UTRs that harbor IRESs [13]. Therefore, R-dys α retaining many IRESs is supposed to have an important physiologic role. Although an ERG abnormality and a red-green color vision defect have been identified in DMD [11,31], the two variants identified in the retina are considered to explain these abnormalities. Further studies analyzing mutations in the 5′-UTR region are required to clarify this.

R-dys α was expressed in the retina and weakly in the cerebellum (Figure 3). This may correlate with synaptic junction formation in these tissues [7,32–35]. No clear abnormalities in the cerebellum of DMD patients have been reported; however, it is possible that a cerebellar phenotype may be revealed as a more precise examination of cerebellar function becomes possible, or when DMD patients can survive for longer than at present. One third of DMD patients show mental retardation [36], but direct genotype-phenotype correlations have not been established for mental retardation in DMD [37]. It would be interesting to analyze alternative splicing of R-dystrophin in relation to mental retardation in DMD.

R-dys β was produced by activated splicing of both introns R1A and R1 from the transcript. This suggests that the same splicing factors facilitate the splicing of both introns. Conversely, in the retina, an unidentified splicing factor may inhibit splicing of intron R1A. Clarification of these factors may facilitate understanding of the physiologic roles of the two variants. The pattern of intron R1A alternative splicing was shown to be key in determining translational activity (Figure 4). IRESs have been reported to provide molecular switches, allowing maintenance of the expression of proteins essential for cell survival or death [13]. Thus, the alternative splicing of intron R1A may act as a molecular switch regulating the expression of R-dystrophin in the retina. The evolution of alternative splicing in the 5′-UTR has been proposed to contribute to the regulation of translation [18]. Our results add another example of an evolutionarily-acquired alternative splicing pathway that regulates translational activity.

ACKNOWLEDGMENTS

We thank Ms. Kanako Yokoyama for her secretarial help. This work was supported in part by a Grant-in-Aid for Scientific Research (B) and Grant-in-Aid for Exploratory Research from the Japan Society for the Promotion of Science; a Health and Labour Sciences Research Grant for Research on Psychiatric and Neurologic Diseases and Mental Health; and a research grant for Nervous and Mental Disorders from the Ministry of Health, Labour and Welfare.

REFERENCES

1. Ahn AH, Kunkel LM. The structural and functional diversity of dystrophin. Nat Genet 1993; 3:283-91. [PMID: 7981747]
2. Nishio H, Takeshima Y, Narita N, Yanagawa H, Suzuki Y, Ishikawa Y, Ishikawa Y, Minami R, Nakamura H, Matsuo M. Identification of a novel first exon in the human dystrophin gene and of a new promoter located more than 500 kb upstream of the nearest known promoter. J Clin Invest 1994; 94:1037-42. [PMID: 8083345]
3. Muntoni F, Torelli S, Ferlini A. Dystrophin and mutations: one gene, several proteins, multiple phenotypes. Lancet Neurol 2003; 2:731-40. [PMID: 14636778]
4. D'Souza VN, Nguyen TM, Morris GE, Karges W, Pillers DA, Ray PN. A novel dystrophin isoform is required for normal retinal electrophysiology. Hum Mol Genet 1995; 4:837-42. [PMID: 7633443]
5. Pillers DA, Bulman DE, Welber RG, Sigesmund DA, Musarella MA, Powell BR, Murphey WH, Westall C, Panton C, Becker LE, Worton RG, Ray PN. Dystrophin expression in the human retina is required for normal function as defined by electroretinography. Nat Genet 1993; 4:82-6. [PMID: 8513332]
6. Rodius F, Claudepierre T, Rosas-Vargas H, Cisneros B, Montanez C, Dreyfus H, Mornet D, Rendon A. Dystrophins in developing retina: Dp260 expression correlates with synaptic maturation. Neuroreport 1997; 8:2383-7. [PMID: 9243645]
7. Ueda H, Baba T, Terada N, Kato Y, Tsukahara S, Ohno S. Dystrophin in rod spherules; submembranous dense regions facing bipolar cell processes. Histochem Cell Biol 1997; 108:243-8. [PMID: 9342618]
8. Schmitz F, Drenckhahn D. Dystrophin in the retina. Prog Neurobiol 1997; 53:547-60. [PMID: 9421835]
9. Prins KW, Humston JL, Mehta A, Tate V, Ralston E, Ervasti JM. Dystrophin is a microtubule-associated protein. J Cell Biol 2009; 186:363-9. [PMID: 19651889]
10. Cibis GW, Fitzgerald KM, Harris DJ, Rothberg PG, Rupani M. The effects of dystrophin gene mutations on the ERG in mice and humans. Invest Ophthalmol Vis Sci 1993; 34:3646-52. [PMID: 8258524]
11. Costa MF, Oliveira AGF, Santana CF, Zatz M, Ventura DF. Red-Green Color Vision Impairment in Duchenne Muscular Dystrophy. Am J Hum Genet 2007; 80:1064-75. [PMID: 17503325]
12. Mironov AA, Fickett JW, Gelfand MS. Frequent alternative splicing of human genes. Genome Res 1999; 9:1288-93. [PMID: 10613851]
13. Pickering BM, Willis AE. The implications of structured 5′ untranslated regions on translation and disease. Semin Cell Dev Biol 2005; 16:39-47. [PMID: 15659338]
14. Miura P, Thompson J, Chakkalakal JV, Holcik M, Jasmin BJ. The utrophin A 5′-untranslated region confers internal ribosome entry site-mediated translational control during regeneration of skeletal muscle fibers. J Biol Chem 2005; 280:32997-3005. [PMID: 16061482]
15. Spriggs KA, Stoneley M, Bushell M, Willis AE. Re-programming of translation following cell stress allows IRES-mediated translation to predominate. Biol Cell 2008; 100:27-38. [PMID: 18072942]
16. Ajay SS, Athey BD, Lee I. Unified translation repression mechanism for microRNAs and upstream AUGs. BMC Genomics 2010; 11:155. [PMID: 20205738]
17. Chatterjee S, Pal JK. Role of 5′- and 3′-untranslated regions of mRNAs in human diseases. Biol Cell 2009; 101:251-62. [PMID: 19275763]
18. Resch AM, Ogurtsov AY, Rogozin IB, Shabalina SA, Koonin EV. Evolution of alternative and constitutive regions of mammalian 5′UTRs. BMC Genomics 2009; 10:162. [PMID: 19371439]
19. Matsuo M, Masumura T, Nishio H, Nakajima T, Kitoh Y, Takumi T, Koga J, Nakamura H. Exon skipping during splicing of dystrophin mRNA precursor due to an intraexon deletion in the dystrophin gene of Duchenne muscular

dystrophy Kobe. J Clin Invest 1991; 87:2127-31. [PMID: 2040695]

20. Surono A, Takeshima Y, Wibawa T, Ikezawa M, Nonaka I, Matsuo M. Circular dystrophin RNAs consisting of exons that were skipped by alternative splicing. Hum Mol Genet 1999; 8:493-500. [PMID: 9949208]
21. Tran VK, Zhang Z, Yagi M, Nishiyama A, Habara Y, Takeshima Y, Matsuo M. A novel cryptic exon identified in the 3′ region of intron 2 of the human dystrophin gene. J Hum Genet 2005; 50:425-33. [PMID: 16133659]
22. Shapiro MB, Senapathy P. RNA splice junctions of different classes of eukaryotes: sequence statistics and functional implications in gene expression. Nucleic Acids Res 1987; 15:7155-74. [PMID: 3658675]
23. Sironi M, Pozzoli U, Cagliani R, Comi GP, Bardoni A, Bresolin N. Analysis of splicing parameters in the dystrophin gene: relevance for physiological and pathogenetic splicing mechanisms. Hum Genet 2001; 109:73-84. [PMID: 11479738]
24. Tokarz SA, Duncan NM, Rash SM, Sadeghi A, Dewan AK, Pillers DA. Redefinition of dystrophin isoform distribution in mouse tissue by RT-PCR implies role in nonmuscle manifestations of duchenne muscular dystrophy. Mol Genet Metab 1998; 65:272-81. [PMID: 9889014]
25. Claudepierre T, Rodius F, Frasson M, Fontaine V, Picaud S, Dreyfus H, Mornet D, Rendon A. Differential distribution of dystrophins in rat retina. Invest Ophthalmol Vis Sci 1999; 40:1520-9. [PMID: 10359335]
26. Ji H, Zhang Y, Zheng W, Wu Z, Lee S, Sandberg K. Translational regulation of angiotensin type 1a receptor expression and signaling by upstream AUGs in the 5′ leader sequence. J Biol Chem 2004; 279:45322-8. [PMID: 15319432]
27. Churbanov A, Rogozin IB, Babenko VN, Ali H, Koonin EV. Evolutionary conservation suggests a regulatory function of AUG triplets in 5′-UTRs of eukaryotic genes. Nucleic Acids Res 2005; 33:5512-20. [PMID: 16186132]
28. Li M, Cheng TS, Ho PW, Chan KH, Mak W, Cheung RT, Ramsden DB, Sham PC, Song Y, Ho SL. −459C>T point mutation in 5′ non-coding region of human GJB1 gene is linked to X-linked Charcot-Marie-Tooth neuropathy. J Peripher Nerv Syst 2009; 14:14-21. [PMID: 19335535]
29. Hellen CU. IRES-induced conformational changes in the ribosome and the mechanism of translation initiation by internal ribosomal entry. Biochim Biophys Acta 2009; 1789:558-70. [PMID: 19539793]
30. Spriggs KA, Cobbold LC, Ridley SH, Coldwell M, Bottley A, Bushell M, Willis AE, Siddle K. The human insulin receptor mRNA contains a functional internal ribosome entry segment. Nucleic Acids Res 2009; 37:5881-93. [PMID: 19654240]
31. Fitzgerald KM, Cibis GW, Giambrone SA, Harris DJ. Retinal signal transmission in Duchenne muscular dystrophy: Evidence for dysfunction in the photoreceptor/depolarizing bipolar cell pathway. J Clin Invest 1994; 93:2425-30. [PMID: 8200977]
32. Pillers DA, Fitzgerald KM, Duncan NM, Rash SM, White RA, Dwinnell SJ, Powell BR, Schnur RE, Ray PN, Cibis GW, Weleber RG. Duchenne/ Becker muscular dystrophy' correlation of phenotype by electroretinography with sites of dystrophin mutations. Hum Genet 1999; 105:2-9. [PMID: 10480348]
33. Banks GB, Fuhrer C, Adams ME, Froehner SC. The postsynaptic submembrane machinery at the neuromuscular junction: requirement for rapsyn and the utrophin/dystrophin-associated complex. J Neurocytol 2003; 32:709-26. [PMID: 15034263]
34. Fort PE, Sene A, Pannicke T, Roux MJ, Forster V, Mornet D, Nudel U, Yaffe D, Reichenbach A, Sahel JA, Rendon A. Kir4.1 and AQP4 associate with Dp71- and utrophin-DAPs complexes in specific and defined microdomains of Muller retinal glial cell membrane. Glia 2008; 56:597-610. [PMID: 18286645]
35. Jastrow H, Koulen P, Altrock WD, Kroger S. Identification of a beta-dystroglycan immunoreactive subcompartment in photoreceptor terminals. Invest Ophthalmol Vis Sci 2006; 47:17-24. [PMID: 16384939]
36. Emery AEH. Duchenne muscular dystrophy. Oxford: Oxford University Press; 1993.
37. Taylor PJ, Betts GA, Maroulis S, Gilissen C, Pedersen RL, Mowat DR, Johnston HM, Buckley MF. Dystrophin gene mutation location and the risk of cognitive impairment in Duchenne muscular dystrophy. PLoS ONE 2010; 5:e8803. [PMID: 20098710]

The print version of this article was created on 6 December 2010. This reflects all typographical corrections and errata to the article through that date. Details of any changes may be found in the online version of the article.

Molecular Genetics and Metabolism 101 (2010) 233–237

Contents lists available at ScienceDirect

Molecular Genetics and Metabolism

journal homepage: www.elsevier.com/locate/ymgme

A Japanese child with asymptomatic elevation of serum creatine kinase shows *PTRF-CAVIN* mutation matching with congenital generalized lipodystrophy type 4

Ery Kus Dwianingsih [a], Yasuhiro Takeshima [a], Kyoko Itoh [b], Yumiko Yamauchi [a], Hiroyuki Awano [a], Rusdy Ghazali Malueka [a], Atsushi Nishida [a], Mitsunori Ota [a], Mariko Yagi [a], Masafumi Matsuo [a,*]

[a] *Department of Pediatrics, Graduate School of Medicine, Kobe University, Kobe, Japan*
[b] *Department of Pathology and Applied Neurobiology, Graduate School of Medical Science, Kyoto Prefectural University of Medicine, Kyoto, Japan*

ARTICLE INFO

Article history:
Received 28 April 2010
Received in revised form 19 June 2010
Accepted 19 June 2010
Available online 1 July 2010

Keywords:
Muscular dystrophy
lipodystrophy
PTRF-CAVIN
CGL4

ABSTRACT

Congenital generalized lipodystrophy (CGL), characterized by generalized absence of adipose tissue, has heterogeneous causes. Recently, a novel type of CGL complicated by muscular dystrophy was categorized as CGL4 caused by PTRF-CAVIN deficiency. However, it is unknown whether CGL4 exhibits clinical abnormalities during the infantile period. Here, we describe the youngest Japanese case of CGL4—a Japanese girl with asymptomatic high serum creatine kinase (CK) levels at 3 months old. She was referred to our hospital at 5 months of age because of her elevated serum CK (2528 IU/L). Generalized absence of adipose tissue was first recognized at 2 years of age. Mutation analysis of genes known to be responsible for CGL1-3 failed to disclose any abnormalities. Instead, analysis of the *PTRF-CAVIN* gene encoding PTRF-CAVIN revealed compound heterozygous mutations, one allele contained an insertion (c.696_697insC) and the other allele harbored a novel nonsense mutation (c.512C>A). Our patient had low serum leptin and adiponectin levels and insulin resistance. Pathological studies on biopsied muscle disclosed mild dystrophic change and highly reduced expression of PTRF-CAVIN. It was concluded that our PTRF-CAVIN deficient patient showed not only CGL but also asymptomatic elevation of serum CK because of her mild muscle dystrophic change.

Introduction

Lipodystrophies are a heterogeneous group of acquired and inherited disorders characterized by selective loss of adipose tissue. Inherited lipodystrophies are rare disorders, which may manifest at birth or may present with fat loss later in life [1]. The extent of fat loss may also vary from being partial to complete [2]. The two main types of inherited lipodystrophies are congenital generalized lipodystrophy (CGL) and familial partial lipodystrophy. CGL is an autosomal recessive disorder in which near total absence of subcutaneous adipose tissue is evident from birth.

CGL patients have been described to show marked muscular appearance with prominent veins, acromegaloid features, acanthosis nigricans, hepatomegaly and umbilical prominence [3]. Metabolic abnormalities related to insulin resistance, such as diabetes mellitus, hyperlipidemia and hepatic steatosis, are evident at a young age and are often difficult to control [3]. However, heterogeneity of CGL was pointed out [4].

Muscle hypertrophy in CGL is suggested to be to the result of the absence of adipose tissue [5]. Muscle dystrophy refers to a group of inherited disorders characterized by muscle weakness, wasting and degeneration. A number of forms of the congenital muscular dystrophies are caused by defects in proteins that are thought to have some relationship to the dystrophin–glycoprotein complex and to the connections between muscle cells and their surrounding cellular structure, including caveolae. Muscle dystrophy is subdivided into nearly twenty sub-types [6]. An elevation of serum creatine kinase (CK) concentration is one of the hallmarks for the identification of muscular dystrophy [7].

Recently, PTRF-CAVIN (polymerase I and transcript release factor/Cavin), has been reported as a new molecule linked to a condition that presents with muscle dystrophy and generalized lipodystrophy [8,9] and PTRF-CAVIN deficiency was categorized as CGL4 (OMIM #613327). So far, four CGL loci have been identified: 1-acylglycerol-3-phosphate-O-acyltransferase 2 (*AGPAT2*), Berardinelli-Seip Congenital Lipodystrophy 2 (*BSCL2*), caveolin-1 (*CAV1*) and *PTRF-CAVIN*. *AGPAT2* plays a critical role in the synthesis of glycerophospholipids and triglycerides required for lipid droplet formation. Another protein, seipin (encoded by *BSCL2* gene), has been found to induce lipid droplet fusion. *CAV1* is an integral component of caveolae and may contribute towards lipid droplet formation [10]. PTRF-CAVIN is essential for the biogenesis of caveolae [11].

CGL4 was first characterized among five non-consanguineous Japanese patients. All but one of the five cases shared one homozygous mutation of in c.696-697insC. Their common clinical findings were

* Corresponding author. Department of Pediatrics, Graduate School of Medicine, Kobe University, 7-5-1 Kusunokicho, Chuo, Kobe 650-0017, Japan. Fax: +81 78 382 6098.
E-mail address: matsuo@kobe-u.ac.jp (M. Matsuo).

1096-7192/$ – see front matter © 2010 Elsevier Inc. All rights reserved.
doi:10.1016/j.ymgme.2010.06.016

muscle weakness, elevated serum CK and absence of adipose tissue when patients were older than 8 years of age. But their clinical findings in their younger period were largely unknown.

Here, we describe a Japanese child with generalized lipodystrophy and asymptomatic elevation in serum CK levels and disclose compound heterozygous mutations of c.696-697insC and a novel nonsense mutation (c.512c>A) in the *PTRF-CAVIN* gene.

Materials and methods

Case

A 3-year-old Japanese female was involved in this study. All clinical materials used in this study were obtained for diagnostic purposes and with informed consent. The institutional review board gave approval for this study.

Gene analysis

Genomic DNA samples were prepared from the patient and her parent's peripheral blood using a standard phenol-chloroform extraction method. Mutations in the dystrophin gene were analyzed using the MLPA DMD kit (SALSA MLPA KIT P034/P035 DMD/Becker, MRC-Holland, Amsterdam, Netherlands) [12]. The coding regions of five genes, *AGPAT2*, *BSCL2*, *CAV1*, *LMNA* and *PTRF-CAVIN* gene, were amplified by PCR using gene-specific primers, as previously reported [8,13–16]. The PCR products were confirmed by electrophoresis on a 2% (w/v) agarose gel. PCR products were purified and sequenced using the BigDye Terminator v1.1 Cycle Sequencing Kit (Applied Biosystems, Foster City, CA) on an automatic DNA sequencer (model ABI Prism 3130 Genetic Analyzer, Applied Biosystems, Foster City, CA). Subcloning sequencing was performed using the pT-7 Blue vector (Novagen, EMD Biosciences, Inc., Darmstadt) as described previously [17].

Histochemical and immunohistochemical analyses of skeletal muscle

Skeletal muscle samples were obtained from the left biceps by biopsy. As a control, a biopsy muscle sample obtained from a 2-year-old boy with congenital myopathy was used. Biopsied muscle specimens were flash-frozen with iso-pentane-cooled in liquid nitrogen. Serial 10-μm-thick frozen sections were analyzed with histochemical staining, including hematoxylin-eosin (H&E), modified Gomori trichrome, NADH-tetrazolium reductase, cytochrome C oxidase, acid phosphatase and alkaline phosphatase, according to the standard protocols. Immunohistochemistry was performed as follows: serial 10-μm-thick frozen muscle sections were fixed in cold acetone for 5 min. After blocking with normal goat serum, sections were incubated with primary antibodies overnight at 4 °C. Antibodies used were anti-caveolin-3 (Santa Cruz Biotechnology, Inc, Santa Cruz, CA), anti-dysferlin (Novocastra Laboratories Ltd, Newcastle upon Tyne, United Kingdom), and anti-PTRF-CAVIN (A301-271A, A301-269A, BETHYL Laboratories, Inc, Montogomery, TX). After six washes in phosphate-buffered saline (PBS), sections were incubated with secondary antibodies, Alexa Fluor 488-labeled goat anti-mouse or anti-rabbit antibodies, at room temperature for 90 min.

Metabolic examination

All chemical examinations including insulin were conducted in the central laboratory of the Kobe University Hospital. Adiponectin and leptin plasma levels were determined by commercially available ELISA (Quantikine; R&D Systems, Oxford, United Kingdom). To monitor obesity status, the body mass index (BMI) was calculated using the following formula: $BMI = w/t^2$ (w: bodyweight in kg; t: height in m) [18].

Results

Patient history

A Japanese girl (KUCG 748) was referred to Kobe University Hospital at the age of 5 months because of elevated serum CK levels. She was born at 40 weeks gestation weighing 2600 g and was the first child of a non-consanguineous healthy Japanese couple. No family history of lipodystrophy or muscular dystrophy was found. At 1 month of age she was diagnosed with congenital hip dislocation. At 3 months old, weak body weight gain (weight: 4550 g, height: 57.3 cm, BMI: 13.9 (normal: 16–18)) was observed and blood chemical examination was conducted to disclose abnormalities in serum CK, AST and ALT levels (2528 (normal: 56–248 IU/L), 67 (normal: 13–31 IU/L) and 62 (normal: 8–34 IU/L), respectively). At 5 months old, lipoatrophy over both extremities and prominent umbilicus were observed. Given that her serum CK levels were still elevated (1594 IU/L), her carrier status for dystrophinopathy was highly supposed. At 2 years and 5 months of age, facial lipoatrophy became marked and congenital generalized lipodystrophy was clinically diagnosed. Her growth and development was normal. Blood chemical examination revealed a high serum CK level (2677 IU/L). Head magnetic resonance imaging and electroencepharogram examinations showed normal results. Although blood glucose was 90 mg/dl, her insulin was elevated to 16 IU/ L, suggesting insulin resistance.

At 3 years of age, a muscle biopsy of her left bicep was performed. Her weight was 13 kg, height was 96 cm and her BMI was 14.1 (Table 1). Physical examination showed generalized absence of subcutaneous fat, but acanthosis nigricans and hepatosplenomegaly were not observed. Cardiac examination revealed neither cardiomegaly nor electrocardiogram abnormalities including long-QT syndrome. Muscle weakness and other muscle symptoms were not seen. No mental retardation was detected. The biochemical investigation revealed that serum insulin was 28 IU/l and blood glucose was 90 mg/dl. Calculated insulin resistance index (HOMA-R) was elevated to 6.2. Leptin and adiponectin were low, 0.8 ng/ml (normal, 10–15 mg/ml) and 2.1 μg/ml (normal, 5–10 μg/ml), respectively. The serum CK concentration remained high at 1729 IU/L. Blood triglyceride

Table 1
Dwianingsih et al.

	Present case	Reported case
Age (year)/sex	3/female	8/female
Mutation	c.512C>A / c.696_697insC	c.696_697insC/ c.696_697insC
Height (cm)/weight (kg)	96/13	124/21.3
BMI	14.1	13.8
Lipodystrophy	Generalized	Generalized
Mental retardation	No	No
Acantosis nigricans	No	No
Hepatosplenomegaly	No	Yes
Umbilical prominence	Yes	No
Endocrine abnormalities	No	Growth hormone
Muscle weakness	No	Distal dominant
Muscle mounding	No	Positive
Muscle hypertrophy	No	Yes
Cardiac symptoms	No	Arrhythmia
Skeletal abnormalities	Hip dislocation	Lordosis, contracture
Other symptoms	No	Constipation
Serum CK (IU/L)	1729	1374
Fasting glucose (mg/dl)	90	75
IRI (U/ml)	28	22.8
HOMA-IR	6.2	9.85
HbA1c (%)	4.7	N/A
Total cholesterol (mg/dl)	138	164
Triglyceride (mg/dl)	115	93
Leptin (ng/ml)	0.8	N/A
Adiponectin (g/ml)	2.1	N/A
Lipid droplet in muscle	No	Yes

N/A: not available.

or cholesterol levels were 171 (normal, 28–149 mg/dl) and 158 mg/dl (normal, 146–219 mg/dl), respectively.

Genetic examination

Because of the asymptomatic elevation of the patient's serum CK levels at the age of 3 months, a carrier status for dystrophinopathy was strongly suggested. Mutation of the dystrophin gene was examined using multiplex ligation-dependant probe amplification (MLPA), but no abnormality was detected. On the diagnosis of congenital general lipodystrophy at the age of 2 years, mutations on *AGPAT2*, *BSCL2* and *CAV1* genes were examined by PCR and direct sequencing, but no mutations were detected in the three genes. In addition, no mutation in the *LMNA* gene, which is responsible for familial partial lipodystrophy, was identified.

Recently, Hayashi et al. [8] disclosed another category of CGL by identifying mutations in the *PTRF-CAVIN* gene in five muscular dystrophy cases complicated with lipodystrophy. Therefore, we conducted a mutation analysis on the *PTRF-CAVIN* gene in our case. Regions of the *PTRF-CAVIN* gene were PCR-amplified and the amplified product was subjected to direct or subcloning sequencing. The exon 2 encompassing region was amplified as two separated fragments. In the fragment of the 3' region of exon 2, the sequencing result became blurred in its 3' region (Fig. 1). Careful examination of sequencing results disclosed that two sequences were rearranged in this blurred region; one sequence completely matched with the wild sequence, but the other was found to have a single nucleotide insertion of a C between c.696 and c.697 (c.696-697insC) (Fig. 1). These results were confirmed by subcloning sequencing (data not shown). This mutation matched with that of the common mutation in a previous study [8]. This insertion shifted the translational reading frame, replacing the last 158 amino acids to an unrelated 191-amino acid sequence. In the previous Japanese study, another mutation of c.515delG was identified in the 5' part of the exon 2 encompassing region [8]. The possibility of c.515delG was closely examined, but no identical mutation was present in the genome of the patient in the current study. Instead, an ambiguous peak was revealed at c.512 where the peak of wild C overlapped with A (Fig. 1). The wild c.512C encoded a TCG codon for serine but c.512A (c.512C>A) encoded for a TAG stop codon (p.S171X). This nucleotide change was confirmed by subcloning sequencing (data not shown). The inheritance patterns of these mutations were examined. c.696-697insC and c.512C>A were inherited from the patient's father and mother, respectively (Fig. 1). The compound heterozygous situation of these two mutations was concluded as the cause of her clinical phenotype.

In addition, a 9-bp insertion (c.1235_1236InsTCTCGGCTC), a known polymorphism [8], was identified in the 3' untranslated region in one allele (data not shown). This 9-bp insertion was also found in one allele of the patient's mother. In this family, the 9-bp insertion segregated with c.512C>A. Taking into consideration that the 9-bp insertion was observed heterozygously in 26% and homozygously in 2% of 200 Japanese control individuals [8], c.512C>A segregating with the 9-bp insertion was considered a relatively new event confined to this family.

Immunohistochemical examination of skeletal muscle

Biopsied muscle showed moderate variation in fiber size, increased fibers with central nuclei, minimal necrosis and regeneration, and mild endomysial fibrosis (Fig. 2A). No lipid droplets were observed. Immunohistochemistry using antibodies against dystrophin (DYS1, DYS2, and DYS3), α- and β-dystroglycan, α-, β-, γ-, and δ-sarcoglycans, merosin, syntrophin and emerin showed no abnormalities. Caveolin-3 was feathery expressed in the cytoplasm and slightly decreased in the sarcolemma (Fig. 2B, F). Immunoreactivity for dysferlin was markedly decreased in the cell membrane (Fig. 2C, G). The expression of PTRF-CAVIN detected by anti-PTRF-CAVIN antibodies (A301-269A and A301-271A) (Fig. 2D, H and E, I, respectively) was significantly reduced in the sarcolemma and the stromal blood vessels as compared with control muscle.

Discussion

This study has examined the youngest Japanese child with mutations in the *PTRF-CAVIN* gene. Compound heterozygous mutations of c.512C>A and c.696-697ins C were identified in the index case

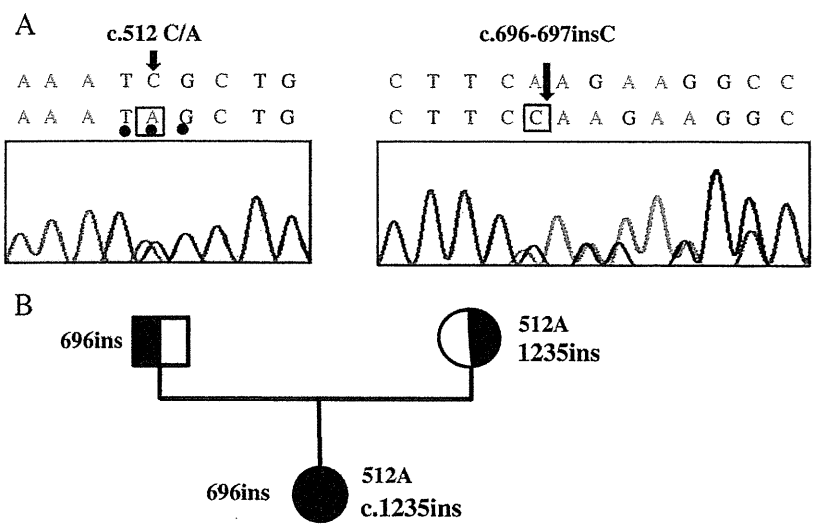

Fig. 1. Nucleotide changes in the *PTRF-CAVIN* gene. (A) Parts of sequencing results are shown. The region encompassing exon 2 of the *PTRF-CAVIN* gene was PCR-amplified as two separate fragments and the PCR-amplified products were directly sequenced. In the 3' part of exon 2 sequencing peaks of nucleotides became overlapped after c.696 (right). The blurred region consisted of a combination of two sequences. One sequence had a completely normal sequence (top line over the sequencing result). The other was found to have a C insertion between 696 and 697 nucleotide (c.696-697insC) (box) (bottom line over the sequencing result). This shifted the translational reading frame. In the sequencing of the 5' part of exon 2, an overlapping of wild C with A nucleotides were observed at c.512 (c.512C/A)(left). This C to A nucleotide change (box) shifted the TCG codon for serine to a stop codon of TAG (c.512C>A) (dots in the bottom line). (B) Pedigree of the family is described. The patient's father is a carrier for the c.696-697insC (half-filled box), while her mother carries both c.512A and c.1235-1236insTCTCGGCTC (half-filled circle). The patient has two responsible mutations (c.696-697insC and c.512A) and one polymorphism (c.1235-1236insTCTCGGCTC) (black circle).

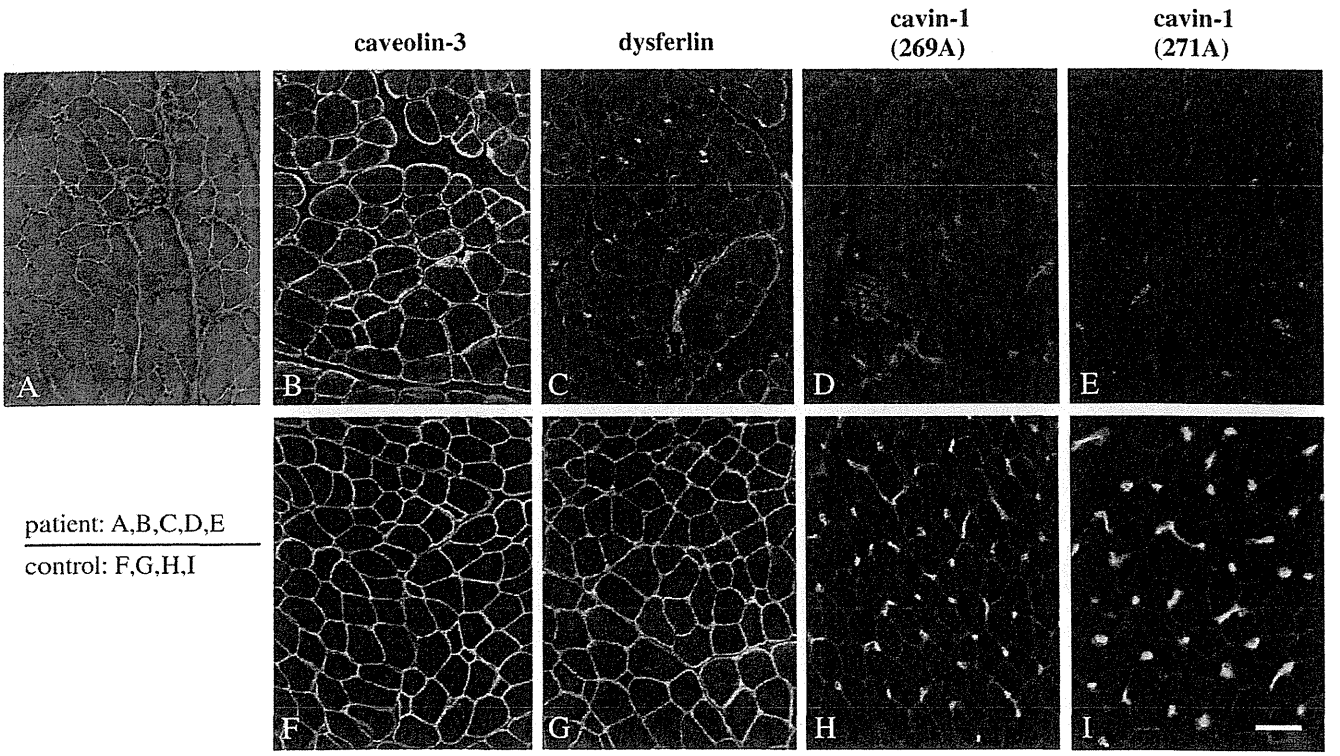

Fig. 2. Histochemical examination of skeletal muscle. Results of histochemical examination are shown from the patient (A, B, C, D and E) and control (F, G, H, and I). Hematoxylin eosin staining of skeletal muscle showed dystrophic changes, including moderate variation in fiber size, increased fibers with central nuclei, few necrotic and regenerating fibers and endomysial fibrosis (A). Intramuscular lipid droplets were not present. Immunoreactivity for caveolin-3 was clearly localized to the sarcolemma of the control muscle (F), whereas it was distributed vaguely in the sarcolemma as well as in the cytoplasm in this patient (B). Dysferlin-immunoreactivity was remarkably decreased in the patient (C) as compared to control muscle (G). Immunoreactivity for PTRF-CAVIN recognized by antibodies of 269A (D, H) or 271A (E, I) was significantly decreased in the patient's muscle (D, E) as compared to the control, which showed distinct PTRF-CAVIN expression in the sarcolemma and the endomysial blood vessels (H, I). Scale bar = 60 μm.

(Fig. 1), and the former and latter mutations were inherited from her mother and father, respectively. Subsequently abnormality of PTRF-CAVIN localization in skeletal muscle was confirmed immunohistochemically (Fig. 2). This is the sixth Japanese case of CGL4 as far as we know [8]. This case had a novel nonsense mutation of c.512C>A. In five reported cases, four homozygous mutations (c.696_697insC) and one compound heterozygous mutation (c.525delG and c.696_697insC) were identified, disclosing two mutations in the *PTRF-CAVIN* gene [8]. The presently reported mutation is the third mutation but the first nonsense mutation. Totally, c.696-697insC was identified in 10 out of 12 alleles, indicating a common mutation in the Japanese cases examined. In our patient, c.512C>A was inherited from the mother together with a 9-bp deletion polymorphism in the 3' UTR (Fig. 1). However, the 3' UTR polymorphism has been reported independently from CGL [8]. Therefore, it was hypothesized that the allele with the 9-bp deletion acquired the nonsense mutation in our family.

To date, the three discovered Japanese mutations are all located in exon 2 of the *PTRF* gene. This clustering of mutations may be explained by further studies on the structure and function of PTRF-CAVIN.

Muscular dystrophy with congenital generalized lipodystrophy is a new category of muscular dystrophy [8,9]. This categorization was based on findings of aged patients who showed a finding compatible with muscular dystrophy. In our case, muscle abnormality was first suggested at 3 months of age by accidental identification of elevated serum CK levels (2528 IU/l). This asymptomatic elevation of serum CK was suggested to be because of the slight dystrophic changes in skeletal muscle at age 3 (Fig. 2). During the follow-up period until the age of 3, there was no complaint of muscle weakness. Though CGL has been described to be recognized at birth or shortly thereafter [10], our case was not recognized based on general adipose tissue deficiency at birth. The patient received medical attention for skeletal abnormalities because of her congenital dislocation of the hip at 1 month of age. Her general deficiency in adipose tissue was brought to our attention at 2 years of age, although poor body weight gain was pointed out at 3 months of age. Compared to the known CGL [10,19], absence of generalized adipose tissue was not initially observed.

To characterize the young Japanese CGL4 case, clinical findings were compared with that of the second youngest case (8 years old) of CGL4 with homozygous c.696_697insC mutation [8] (Table 1). Both cases showed similar clinical findings of low BMI, and generalized lipodystrophy without complications of hypertriglyceridemia or hypercholesterolemia. They did not show mental retardation or acanthosis nigricans. These two cases had differing skeletal abnormalities: congenital hip dislocation in our case but lordosis and contracture in the other case. High serum CK levels were common to both cases (Table 1). Pathological findings including lipid droplets in skeletal muscle were more severe in the 8-year-old patient case, indicating progressive muscle wasting and weakness. In addition, it is suggested that cardiac muscle is also affected by CGL4, as the 8-year-old patient showed cardiac arrhythmia and life-threatening arrhythmia had occurred in older CGL4 cases [9].

PTRF-CAVIN is thought to play an important role in the process of caveolin protein stabilization in caveolae [11,20]. Animals lacking PTRF-CAVIN have no morphologically detectable caveolae in all cell types examined and show dyslipidemia and glucose intolerance [21]. In humans, CGL4 causes secondary deficiency of caveolins, leading to malformation of caveolae in cell membranes [8]. This could have consequences for the regulation of insulin signaling in adipocytes, as caveolae are known to concentrate insulin receptors along their margins [22]. In fact, both CGL4 cases showed insulin resistance as observed by elevated HOMA-IR at a young age (Table 1). This insulin

resistance is suggested to be the result of caveolae abnormalities caused by CGL4 [22].

In the absence of adipocytes designed for synthesis and storage of neutral lipids, dietary lipids accumulate in non-adipose tissues such as the liver and muscle, leading to cellular toxicity and metabolic abnormalities [10]. Our youngest case did not show hepatomegaly or lipid drops in skeletal muscle (Fig. 2), whereas the 8-year-old case showed hepatosplenomegaly and lipid droplets in skeletal muscle (Table 1). Therefore, it appears that lipid accumulation occurs over long periods of time in these tissues.

The adipocytes also secrete a variety of biologically active substances such as leptin and adiponectin [23]. Our case showed low levels of leptin and adiponectin (Table 1) [24,25]. It was pointed out that abnormalities in leptin and adiponectin were already apparent at the age of 3 [26]. Although leptin and adiponectin are both secreted by adipocytes, they show different behavior, leptin levels being related to adipose tissue mass, and adiponectin levels to insulin sensitivity [27]. Redefining lipodystrophy as an adipokine deficiency syndrome leads to the hypothesis that supplementation of one or more adipokines may improve metabolic outcomes in lipodystrophy [28]. To prevent the development of metabolic complications, leptin therapy would be considered in our case in the future [29,30].

Acknowledgments

We would like to thank Ms. Kanako Yokoyama for her administrative assistance. This work was supported by a Grant-in-Aid for Scientific Research (B) and Grant-in-Aid for Exploratory Research from the Japan Society for the Promotion of Science, a Health and Labour Sciences Research Grant for Research on Psychiatric and Neurological Diseases and Mental Health, and a research grant for Nervous and Mental disorders from the Ministry of Health, Labour, and Welfare.

References

[1] A.K. Agarwal, A. Garg, Genetic basis of lipodystrophies and management of metabolic complications, Annu. Rev. Med. 57 (2006) 297–311.
[2] V. Simha, A. Garg, Inherited lipodystrophies and hypertriglyceridemia, Curr. Opin. Lipidol. 20 (2009) 300–308.
[3] A.K. Agarwal, A. Garg, Genetic disorders of adipose tissue development, differentiation, and death, Annu. Rev. Genomics Hum. Genet. 7 (2006) 175–199.
[4] A. Rajab, K. Heathcote, S. Joshi, S. Jeffery, M. Patton, Heterogeneity for congenital generalized lipodystrophy in seventeen patients from Oman, Am. J. Med. Genet. 110 (2002) 219–225.
[5] K.B. Gomes, V.C. Pardini, A.P. Fernandes, Clinical and molecular aspects of Berardinelli-Seip Congenital Lipodystrophy (BSCL), Clin. Chim. Acta 402 (2009) 1–6.
[6] L. Costanza, M. Moggio, Muscular dystrophies: histology, immunohistochemistry, molecular genetics and management, Curr. Pharm. Des. (2009).
[7] J.C. Reijneveld, N.C. Notermans, W.H. Linssen, P.R. Bar, J.H. Wokke, Hyper-CK-aemia revisited, Neuromuscul. Disord. 11 (2001) 163–164.
[8] Y.K. Hayashi, C. Matsuda, M. Ogawa, K. Goto, K. Tominaga, S. Mitsuhashi, Y.E. Park, I. Nonaka, N. Hino-Fukuyo, K. Haginoya, H. Sugano, I. Nishino, Human PTRF mutations cause secondary deficiency of caveolins resulting in muscular dystrophy with generalized lipodystrophy, J. Clin. Invest. 119 (2009) 2623–2633.
[9] A. Rajab, V. Straub, L.J. McCann, D. Seelow, R. Varon, R. Barresi, A. Schulze, B. Lucke, S. Lutzkendorf, M. Karbasiyan, S. Bachmann, S. Spuler, M. Schuelke, Fatal cardiac arrhythmia and long-QT syndrome in a new form of congenital generalized lipodystrophy with muscle rippling (CGL4) due to PTRF-CAVIN mutations, PLoS Genet. 6 (2010) e1000874.
[10] A. Garg, A.K. Agarwal, Lipodystrophies: disorders of adipose tissue biology, Biochim. Biophys. Acta 1791 (2009) 507–513.
[11] L. Liu, P.F. Pilch, A critical role of cavin (polymerase I and transcript release factor) in caveolae formation and organization, J. Biol. Chem. 283 (2008) 4314–4322.
[12] Y. Okizuka, Y. Takeshima, H. Awano, Z. Zhang, M. Yagi, M. Matsuo, Small mutations detected by multiplex ligation-dependant probe amplification of the dystrophin gene, Genet. Test Mol. Biomark. 13 (2009) 427–431.
[13] J. Magre, M. Delepine, E. Khallouf, T. Gedde-Dahl Jr., L. Van Maldergem, E. Sobel, J. Papp, M. Meier, A. Megarbane, A. Bachy, A. Verloes, F.H. d'Abronzo, E. Seemanova, R. Assan, N. Baudic, C. Bourut, P. Czernichow, F. Huet, F. Grigorescu, M. de Kerdanet, D. Lacombe, P. Labrune, M. Lanza, H. Loret, F. Matsuda, J. Navarro, A. Nivelon-Chevalier, M. Polak, J.J. Robert, P. Tric, N. Tubiana-Rufi, C. Vigouroux, J. Weissenbach, S. Savasta, J.A. Maassen, O. Trygstad, P. Bogalho, P. Freitas, J.L. Medina, F. Bonnicci, B.I. Joffe, G. Loyson, V.R. Panz, F.J. Raal, S. O'Rahilly, T. Stephenson, C.R. Kahn, M. Lathrop, J. Capeau, Identification of the gene altered in Berardinelli-Seip congenital lipodystrophy on chromosome 11q13, Nat. Genet. 28 (2001) 365–370.
[14] A.K. Agarwal, A. Garg, Congenital generalized lipodystrophy: significance of triglyceride biosynthetic pathways, Trends Endocrinol. Metab. 14 (2003) 214–221.
[15] H. Cao, L. Alston, J. Ruschman, R.A. Hegele, Heterozygous CAV1 frameshift mutations (MIM 601047) in patients with atypical partial lipodystrophy and hypertriglyceridemia, Lipids Health Dis. 7 (2008) 3.
[16] D. Fatkin, C. MacRae, T. Sasaki, M.R. Wolff, M. Porcu, M. Frenneaux, J. Atherton, H.J. Vidaillet Jr., S. Spudich, U. De Girolami, J.G. Seidman, C. Seidman, F. Muntoni, G. Muehle, W. Johnson, B. McDonough, Missense mutations in the rod domain of the lamin A/C gene as causes of dilated cardiomyopathy and conduction-system disease, N Engl J. Med. 341 (1999) 1715–1724.
[17] A. Surono, V.K. Tran, Y. Takshima, H. Wada, M. Yagi, M. Takagi, M. Koizumi, M. Matsuo, Chimeric RNA/ethylene bridged nucleic acids promote dystrophin expression in myocytes of Duchenne muscular dystrophy by inducing skipping of the nonsense-mutation-encoding exon, Hum. Gene Ther. 15 (2004) 749–757.
[18] T.J. Cole, M.C. Bellizzi, K.M. Flegal, W.H. Dietz, Establishing a standard definition for child overweight and obesity worldwide: international survey, BMJ 320 (2000) 1240–1243.
[19] A. Nishiyama, M. Yagi, H. Awano, Y. Okizuka, T. Maeda, S. Yoshida, Y. Takeshima, M. Matsuo, Two Japanese infants with congenital generalized lipodystrophy due to BSCL2 mutations, Pediatr. Int. 51 (2009) 775–779.
[20] R. Chadda, S. Mayor, PTRF triggers a cave in, Cell 132 (2008) 23–24.
[21] L. Liu, D. Brown, M. McKee, N.K. Lebrasseur, D. Yang, K.H. Albrecht, K. Ravid, P.F. Pilch, Deletion of Cavin/PTRF causes global loss of caveolae, dyslipidemia, and glucose intolerance, Cell Metab. 8 (2008) 310–317.
[22] M. Foti, G. Porcheron, M. Fournier, C. Maeder, J.L. Carpentier, The neck of caveolae is a distinct plasma membrane subdomain that concentrates insulin receptors in 3T3-L1 adipocytes, Proc. Natl. Acad. Sci. USA 104 (2007) 1242–1247.
[23] R.A. Hegele, T.R. Joy, S.A. Al-Attar, B.K. Rutt, Thematic review series: Adipocyte Biology. Lipodystrophies: windows on adipose biology and metabolism, J. Lipid Res. 48 (2007) 1433–1444.
[24] R. Nishimura, H. Sano, T. Matsudaira, A. Morimoto, Y. Miyashita, T. Shirasawa, A. Kokaze, N. Tajima, Changes in body mass index, leptin and adiponectin in Japanese children during a three-year follow-up period: a population-based cohort study, Cardiovasc. Diabetol. 8 (2009) 30.
[25] G. Iniguez, N. Soto, A. Avila, T. Salazar, K. Ong, D. Dunger, V. Mericq, Adiponectin levels in the first two years of life in a prospective cohort: relations with weight gain, leptin levels and insulin sensitivity, J. Clin. Endocrinol. Metab. 89 (2004) 5500–5503.
[26] B. Antuna-Puente, E. Boutet, C. Vigouroux, O. Lascols, L. Slama, M. Caron-Debarle, E. Khallouf, C. Levy-Marchal, J. Capeau, J.P. Bastard, J. Magre, Higher adiponectin levels in patients with Berardinelli–Seip congenital lipodystrophy due to seipin as compared with 1-acylglycerol-3-phosphate-o-acyltransferase-2 deficiency, J. Clin. Endocrinol. Metab. 95 (2010) 1463–1468.
[27] M. Matsubara, S. Maruoka, S. Katayose, Inverse relationship between plasma adiponectin and leptin concentrations in normal-weight and obese women, Eur. J. Endocrinol. 147 (2002) 173–180.
[28] E.A. Oral, J.L. Chan, The rationale for leptin-replacement therapy as a treatment for severe lipodystrophy, Endocr. Pract. 16 (2010) 1–35.
[29] A.Y. Chong, B.C. Lupsa, E.K. Cochran, P. Gorden, Efficacy of leptin therapy in the different forms of human lipodystrophy, Diabetologia 53 (2010) 27–35.
[30] S. Bluher, S. Shah, C.S. Mantzoros, Leptin deficiency: clinical implications and opportunities for therapeutic interventions, J. Investig. Med. 57 (2009) 784–788.

Journal of Human Genetics (2010), 1–6

www.nature.com/jhg

ORIGINAL ARTICLE

Contemporary retrotransposition of a novel non-coding gene induces exon-skipping in dystrophin mRNA

Hiroyuki Awano, Rusdy Ghazali Malueka, Mariko Yagi, Yo Okizuka, Yasuhiro Takeshima and Masafumi Matsuo

Non-autonomous retrotransposon-mediated mobilizations of the Alu family are known pathogenic mechanisms of human disease. Here, we report a pathogenic, contemporary, non-autonomous retrotransmobilization of part of a novel non-coding gene into the *dystrophin* gene. In a Japanese Duchenne muscular dystrophy patient, a 330-bp-long *de novo* insertion was identified in exon 67 of dystrophin. The insertion induced exon 67-skipping in the dystrophin mRNA, creating a premature stop codon. The sequence of the insertion had certain characteristics of retrotransposons: an antisense polyadenylation signal accompanied by a poly(T) sequence and a target site duplication. The insertion site matched the consensus recognition sequence for the L1 endonuclease, indicating a retrotransposon-mediated event, although the inserted sequence did not match any known retrotransposons. The origin of the inserted sequence was mapped to a gene-poor region of chromosome 11. The inserted fragment was expressed in multiple human tissue RNAs, indicating that it is a novel transcript. The full length of the transcript was cloned and showed no meaningful protein coding ability.
Journal of Human Genetics advance online publication, 9 September 2010; doi:10.1038/jhg.2010.111

Keywords: Duchenne muscular dystrophy; dystrophin; exon-skipping; non-coding gene; retrotransposon

INTRODUCTION

Mobile DNA elements are discrete DNA sequences that have the remarkable ability to transport or duplicate themselves to other regions of the genome. Mobile elements can be divided into two different classes based on how they duplicate themselves within the genome.[1,2] DNA transposons mobilize through a DNA intermediate, typically using a so-called 'cut-and-paste' mechanism. Retrotransposons mobilize through RNA and proceed via a 'copy-and-paste' mechanism. In this process, an RNA copy is first generated from the original retrotransposon and is subsequently reverse transcribed back into DNA using the enzyme reverse transcriptase. cDNA is then inserted into a new location in the genome, sometimes disrupting host gene function.[3–5]

Retrotransposons can be further subdivided into those elements that are autonomous, meaning that they encode their own replication machinery (for example, long interspersed nuclear element 1: L1 or LINE1),[6] and those elements that are non-autonomous, such as the Alu family.[2] Non-autonomous retrotransposons borrow the enzymatic machinery required for their propagation from L1 elements. L1 endonuclease-dependent retrotransposition has been reported to cause many human genetic diseases.[7]

Processed pseudogenes are another retrotransposable element resulting from the random integration of reverse-transcribed mature RNA molecules into genomes. They are characterized by a lack of introns, the presence of a poly(A) tail and the presence of flanking direct repeats.[8] This gene retrotransposition may arise as a by-product of L1 retrotransposition.[9] Recently, an ancient retrotranspositional insertion of a transcript from chromosome 6 (chromosome 6 open-reading frame 68) has been shown to disrupt the *SLC25A13* gene.[10] Contemporary retrotransposition of a gene transcript has never been shown to cause a genetic disease.

Mutations in the *dystrophin* gene, the largest human gene spreading over 2500 kb on the short arm of the X chromosome, cause Duchenne muscular dystrophy (DMD), the most common inherited muscular disease affecting one in every 3500 male subjects. Although deletions removing one or more exon of the gene have been reported as the most common mutation, more than 200 mutations have been identified in the *dystrophin* gene (http://www.dmd.nl/). To date, retrotranspositional insertions into this gene have been reported in four cases. In our previous Japanese study, an L1 insertion was identified in one Japanese DMD patient.[11] All three other insertions were derived from L1 retrotransposons.[12–14]

Here, we identify a contemporary retrotranspositional insertion of a novel non-coding gene from chromosome 11 into exon 67 of the *dystrophin* gene in a Japanese DMD patient. This is a novel retrotransposon-mediated transmobilization that causes human disease.

MATERIALS AND METHODS

Case

The proband (KUCG732) was a 4-year-old Japanese boy. He had no family history of neuromuscular disease. At 3 years old, his serum creatine kinase level

Department of Pediatrics, Graduate School of Medicine, Kobe University, Kobe, Japan
Correspondence: Professor M Matsuo, Department of Pediatrics, Graduate School of Medicine, Kobe University, 7-5-1 Kusunokicho, Chuo, Kobe 650-0017, Japan.
E-mail: matsuo@kobe-u.ac.jp
Received 21 April 2010; revised 6 August 2010; accepted 9 August 2010

was found to be high (14 780 IU l^{-1}) on blood chemical examination. At 4 years old, a muscle biopsy was performed and immunohistochemical examination, using three dystrophin monoclonal antibodies that recognize three different epitopes, found an absence of dystrophin staining, and the DMD diagnosis was confirmed. Informed consent was obtained from his parents for molecular analysis and the study was approved by the ethics committees of Kobe University School of Medicine (approval no. 28 in 1998).

Methods

Mutation analysis. The patient's genomic DNA was extracted from peripheral blood. Each of the 79 exons of the *dystrophin* gene was polymerase chain reaction (PCR) amplified as described previously.[15] The region encompassing exon 67 was amplified using the forward primer DMD-67U (5′-GAAGTA ACCCCACTACTGTGGAA-3′) and the reverse primer DMD-67L (5′-AAACGA AGCTCTGTGGGTTT-3′).

The dystrophin mRNA expressed in the skeletal muscle was examined by reverse transcription PCR (RT-PCR) as described previously.[16] Briefly, total RNA was isolated from thinly sliced (6-μm) sections of frozen muscle using Isogen (Nippon Gene, Toyama, Japan). After synthesizing cDNA with reverse transcriptase (Invitrogen Corp., Carlsbad, CA, USA), a fragment extending from exons 64 to 68 was amplified using a forward primer corresponding to a segment of exon 64 (c64f, 5′-CTCCGAAGACTGCAGAAGGC-3′) and a reverse primer complementary to a segment of exon 68 (5D, 5′-TTTCTGCAGCCA CTCT-3′) as described previously.[17]

The PCR-amplified products were electrophoresed on agarose gels. Purified PCR products were subjected to sequencing either directly or after subcloning into the pT7 blue T vector (Novagen, Madison, WI, USA).

Transcript analysis. A fragment covering the inserted sequence was amplified by RT-PCR from human tissue RNAs (Human Total RNA Panel; Clontech, Mountain View, CA, USA). First-strand cDNA synthesis was carried out with 3 μg of RNA using SuperScript II reverse transcriptase (Invitrogen Corp.). To amplify the fragment covering the inserted sequence, the forward primer awa11q3Lf (5′-GCCTCTGGATCAGGAAGAGC-3′) and the reverse primer awa11q3Rr (5′-TTTTTGAAATTTGAAGCATTTTTCC-3′) were used. Thirty-five PCR cycles were performed in a mixture as described before,[17] using the following conditions: initial denaturation at 94 °C for 4 min, subsequent denaturation at 94 °C for 1 min, annealing at 60 °C for 1 min and extension at 72 °C for 1 min. The final extension reaction was carried out at 72 °C for 1 min. An aliquot of amplified DNA was electrophoresed on a 3% agarose gel and stained with ethidium bromide along with a low-molecular-weight DNA standard (ϕ174X–*Hae*III digest; Takara Bio, Shiga, Japan). In addition, a fragment of the glyceraldehyde 3-phosphate dehydrogenase (*GAPDH*) gene was also amplified using two primers: the forward primer GAPDH-F106 (5′-CCCTTCATTGACCTCAAC-3′) and the reverse primer GAPDH-R407 (5′-TTCACACCCATGACGAAC-3′), as described before. These PCR products were verified by sequencing.

Cloning of the novel transcript. To obtain the 5′ end of the novel transcript, 5′-rapid amplification of cDNA ends (5′-RACE) was performed using the 5′-RACE System (version 2.0; Invitrogen Corp.). Single-stranded cDNA was synthesized from brain RNA (Clontech) using a gene-specific primer, GSP1 (5′-TGAAATTTGAAGCATTTTTCCAA-3′). A homopolymeric T-tail was added to the 3′ end of the cDNA using terminal deoxynucleotidyl transferase and dCTP. The dC-tailed cDNA was amplified with the gene-specific primer, GSP2 (5′-GGCTGTGAATAATAGCATTCT-3′), and the cassette primer, Abridged Anchor (5′-GGCCACGCGTCGACTAGTACGGGGGGGGGG-3′). The resulting product was re-amplified in a second round of PCR using the primers nestedGSP (5′-CCACCAAACTGTTAAACTCA-3′) and AUAP (5′-GGC CACGCGTCGACTAGTAC-3′). PCR products were separated by agarose gel electrophoresis and subjected to subcloning and sequencing.

DNA sequencing. DNA sequencing was performed using the BigDye 2.0 or 3.1 Terminator Cycle Sequencing kit (Applied Biosystems, Foster City, CA, USA). PCR products for sequencing were either gel-purified and/or cloned into the pT7 blue T vector (Novagen) using the TOPO TA Cloning kit (Invitrogen Corp.). The primers used for sequencing PCR products were identical to the primers used for amplification of the corresponding targets. Sequencing of PCR fragments cloned into the pT7 blue T vector was performed using the forward primer PT7-F (5′-CTATAGGGAAAGCTTGCATGC-3′) and reverse primer PT7-R (5′-GTTTTCCCAGTCACGACGTTG-3′). Sequencing was performed on an ABI 310 capillary sequencer (Applied Biosystems).

Database searches and multiple sequence alignments. Homology searches were conducted using the Basic Local Alignment Search Tool (http://blast.ncbi.nlm.nih.gov/) at the nucleotide, transcript or protein level in GenBank (http://www.ncbi.nlm.nih.gov/genbank/), Refseq_rna (http://www.ncbi.nlm.nih.gov/RefSeq/), dbEST (http://www.ncbi.nlm.nih.gov/projects/dbEST/), Swissprot (http://www.expasy.org/sprot/) and Refseq_protein (http://www.ncbi.nlm.nih.gov/RefSeq/). Micro-RNA analysis was performed using miRBase (http://mirbase.org/). DNA sequences encompassing the inserted sequence were analyzed for repetitive elements using the RepeatMasker web server (www.repeatmasker.org) with Repbase (http://www.girinst.org/repbase/) database. The core promoter was analyzed using Genetyx, version 8.2.0 (Genetyx Corp., Osaka, Japan).

RESULTS

To identify the responsible mutation in the *dystrophin* gene in the index case, all 79 exons of the *dystrophin* gene were PCR amplified using primers in the flanking introns. All exons except exon 67 could be amplified at their normal lengths. The amplified region encompassing exon 67 was obtained as a fragment larger than the same region amplified from the patient's father or mother (Figure 1a). Sequencing of the amplified product (Figure 1b) revealed that the 5′ portion of the sequence was identical to the normal sequence until the eighth nucleotide of exon 67 (c.9657C), but this was followed by approximately 330 bp of unknown sequence. The unknown sequence was followed by the 3′ portion of exon 67, beginning at c.9655T, and the amplified portion of intron 67. This indicated that there was an approximately 330-bp insertion mutation in exon 67. As the patient's mother displayed only one normal-sized amplicon for this region, as did his father (Figure 1a), she was deemed a non-carrier for this mutation. Therefore, we concluded that the insertion event occurred *de novo* in the patient.

The impact of the large insertion on splicing was examined by RT-PCR amplification of dystrophin mRNA obtained from skeletal muscle. When the region extending from exons 64 to 68 was amplified, the amplified product was shorter than expected (Figure 2). Sequencing of this product showed that the 3′ end of exon 66 joined directly to the 5′ end of exon 68, indicating complete exon 67-skipping. As the result of a frame shift, a premature stop codon was created at the second codon in exon 68. We concluded that the insertion caused exon 67-skipping, which led to the DMD phenotype.

To identify the insertion, we examined the inserted sequence and discovered two important characteristics: (1) TTC trinucleotides from c.9655 to 9657 were present at both ends, indicating that TTC was the target site for duplication (Figure 1b); and (2) the inserted sequence had an approximately 115-bp stretch of T (Figure 1b). These hallmarks indicated that the inserted fragment was a retrotransposed element. In addition, the remaining 212 bp of the inserted sequence had the reverse sequence of the polyadenylation signal (TTTATT) at the 26th nucleotide from the end (Figure 1b). However, a homology search for the 212-bp unknown sequence revealed no homology in any retrotransposon or transcript sequence database. Instead, we found a single genomic sequence on the long arm of chromosome 11 (11q22) that the complementary sequence of the 212-bp insertion matched perfectly (9041614–9041825, GenBank accession no., NT_033899.8) (Figure 3). As expected, a poly(A) stretch complementary to the poly(T) was not present in this genomic region. These results indicated that the inserted fragment was a reverse-transcribed product from a transcript with a poly(A) tail.

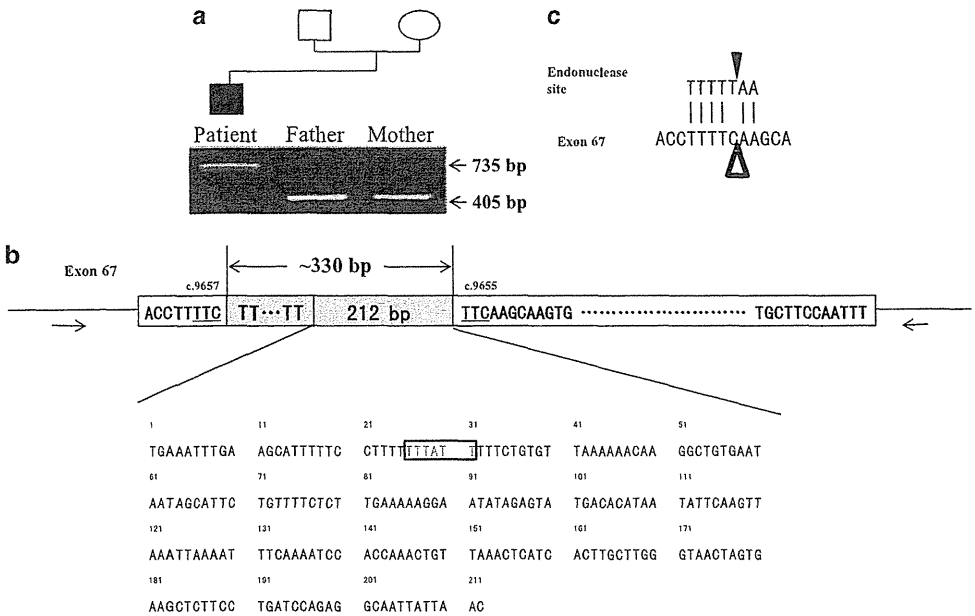

Figure 1 Analysis of the exon 67-encompassing region of the *dystrophin* gene. (**a**) Polymerase chain reaction (PCR) amplification of the exon 67-encompassing region. From the index patient, one clear product was obtained, but its size (735 bp) was larger than that amplified from his father or mother (405 bp). The pedigree of the family is also shown. (**b**) Schematic description of the exon 67-encompassing region of the patient. Open bars indicate the separated exon 67. The horizontal lines indicate introns. Horizontal arrows indicate the location and directions of primers. The shaded bar indicates a ~330-bp inserted sequence. The 5′ portion of exon 67 ended at the eighth nucleotide (c.9657), and the 3′ portion started at the sixth nucleotide of exon 67 (c.9655). The underlined TTC appears twice, at the end of the 5′ portion of exon 67 and at the beginning of the 3′ portion of exon 67. The inserted sequence is divided into two parts: the first has a poly(T) stretch of approximately 115 bp and the second has a unique 212-bp sequence that is described below. The candidate polyadenylation signal (TTTATT) is boxed. (**c**) Sequences around the insertion site. The consensus sequence for the L1 endonuclease site is shown on the upper line. The wild-type sequence of exon 67 is described on the lower line. Vertical lines indicate nucleotide matches. The filled triangle indicates the cleavage site. The open triangle indicates the site of the insertion.

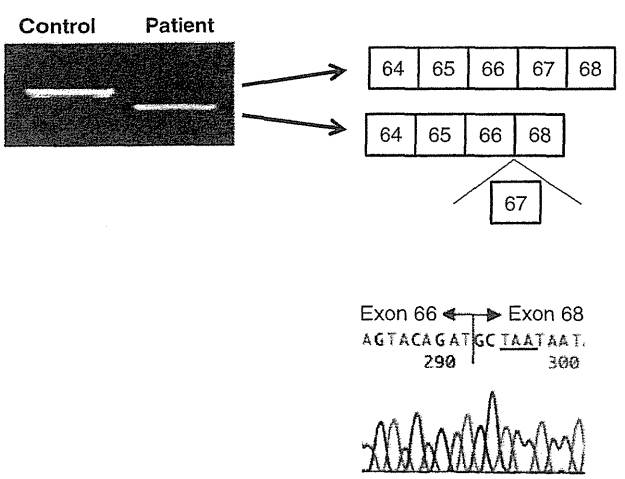

Figure 2 Reverse transcription-polymerase chain reaction (RT-PCR) amplification of dystrophin exons 64–68. RT-PCR products encompassing dystrophin exons 64–68 are shown (left). The size of the product obtained from the patient was smaller than the expected 582 bp (control). On the right-hand side is a schematic representation of the exon organization of the amplified fragment. Exon 67 has been completely removed from the dystrophin cDNA in the patient. The lower panel shows part of the sequence at the junction of exons 66 and 68. The 3′ terminal sequence of exon 66 (GAT) is directly joined to the 5′ end of exon 68 (GCT). The underlined sequence represents a stop codon (TAA).

When the sequence around the inserted site in exon 67 was examined, TTTTCAA, which is highly similar to the consensus sequence for the L1 endonuclease cleavage site (TTTTT/AA; '/' denotes the cleavage site), was found in the wild-type exon 67 sequence (Figure 1c). These sequences differed by only one nucleotide, with the fifth T replaced with the other pyrimidine nucleotide, C (underlined). Remarkably, the insertion was present at exactly the endonuclease cleavage site (Figure 1c). This indicated that an L1 endonuclease cut at TTTTC/AA creating the TTC target duplication. From the characteristics of the inserted sequence and the insert site sequence, we concluded that the insertion event was an L1-mediated retrotransposition.

Our findings strongly suggested that the source region on chromosome 11 is actively transcribed and thus can be reverse transcribed. As a database search failed to disclose the presence of this transcript in the human transcriptome, we assumed that the transcribed sequence has gone undetected because of a high tissue or developmental specificity. To observe expression of the source region, RT-PCR amplification of a fragment of the inserted segment was conducted using 10 human tissue RNAs (Figure 4). Remarkably, the expected product (206 bp) was observed clearly in the brain, thyroid, placenta, skeletal muscle and testis, and faintly in the heart, lung and kidney. The validity of the PCR products was confirmed by sequencing. No product was observed from the liver and bone marrow. Accordingly, no product was obtained from any of the 10 examined tissues (data not shown) when the PCR was conducted without the reverse transcription step. This indicates that the inserted sequence was present as a transcript in these tissues.